



**HAL**  
open science

# Toward a direct combination of space-geodetic techniques at the measurement level: Methodology and main issues

David Coulot, Philippe Bério, Richard Biancale, Sylvain Loyer, Laurent Soudarin, Anne-Marie Gontier

## ► To cite this version:

David Coulot, Philippe Bério, Richard Biancale, Sylvain Loyer, Laurent Soudarin, et al.. Toward a direct combination of space-geodetic techniques at the measurement level: Methodology and main issues. *Journal of Geophysical Research : Solid Earth*, 2007, 112, pp.5410. 10.1029/2006JB004336 . hal-03732756

**HAL Id: hal-03732756**

**<https://hal.science/hal-03732756v1>**

Submitted on 22 Aug 2022

**HAL** is a multi-disciplinary open access archive for the deposit and dissemination of scientific research documents, whether they are published or not. The documents may come from teaching and research institutions in France or abroad, or from public or private research centers.

L'archive ouverte pluridisciplinaire **HAL**, est destinée au dépôt et à la diffusion de documents scientifiques de niveau recherche, publiés ou non, émanant des établissements d'enseignement et de recherche français ou étrangers, des laboratoires publics ou privés.

Copyright

## Toward a direct combination of space-geodetic techniques at the measurement level: Methodology and main issues

D. Coulot,<sup>1,2</sup> P. Berio,<sup>2</sup> R. Biancale,<sup>3</sup> S. Loyer,<sup>4</sup> L. Soudarin,<sup>5</sup> and A.-M. Gontier<sup>6</sup>

Received 9 February 2006; revised 26 October 2006; accepted 6 December 2006; published 12 May 2007.

[1] In the framework of the activities of the Combination Research Centers (CRC) of the International Earth Rotation and Reference Systems Service (IERS), the French Groupe de Recherche en Géodésie Spatiale (GRGS) studies the benefit of combining space-geodetic techniques (Doppler orbitography and radiopositioning integrated by satellite, GPS, satellite laser ranging, and very long baseline interferometry) at the observational level. This combination aims to produce a global and consistent solution for Earth orientation parameters (EOPs), polar motion  $x_p$  and  $y_p$ , and universal time  $UT1$  with a 1-day or a 6-hour sampling, as well as weekly station positions. In this paper we present a methodology for multitechnique combination at the observational level. We process the measurements of the four techniques over a 1-year period (the year 2002) in order to illustrate and validate our method. All techniques are processed with the same computational framework, thus with the same models and a priori values for parameters. By using the same software and conventions, we avoid inconsistencies in individual computations. We process each technique individually and inside the combination. The comparison between these solutions is a way of analyzing the power of our method even if the actual status of our software does not reproduce the state-of-the-art analyses of each technique. However, we produce an analysis of the quality of our individual computations so that readers can get an informed appreciation of the current capabilities of our software. Finally, we present the capability of such combinations in terms of accuracy and precision, we underline the main issues of our method and propose solutions to solve them in the future.

**Citation:** Coulot, D., P. Berio, R. Biancale, S. Loyer, L. Soudarin, and A.-M. Gontier (2007), Toward a direct combination of space-geodetic techniques at the measurement level: Methodology and main issues, *J. Geophys. Res.*, *112*, B05410, doi:10.1029/2006JB004336.

### 1. Introduction

[2] One of the ultimate goals of space geodesy is to estimate point positions on the Earth's surface as accurately as possible. Space-geodetic techniques also provide positions of the Earth's rotation axis with respect to the crust and values linked to the Earth's rotation at given dates. These quantities are major references for all geodetic and astronomical applications. Indeed, anyone who wants to observe an object in space (star, planet, artificial satellite, etc.) from Earth often needs to position it with respect to a ground instrument. This positioning is carried out through two reference frames: the International Celestial Reference Frame (ICRF) [Arias *et al.*, 1995] and the International

Terrestrial Reference Frame (ITRF) [Altamimi *et al.*, 2002a]. The transformation between these terrestrial and celestial frames is directly linked to Earth rotation phenomena. In particular, this transformation makes use of Earth orientation parameters (EOPs) provided as daily time series by the International Earth Rotation and Reference Systems Service (IERS) [Gambis, 2004].

[3] All these fundamental geodetic products are computed by combinations of space-geodetic techniques (except for ICRF, which is only computed with very long baseline interferometry (VLBI)). Indeed, combining techniques takes advantage of the capabilities of each individual technique. For example, satellite laser ranging (SLR) is known as the most accurate technique for assessing geocenter motion. However, this technique depends on weather conditions and its network is largely deficient in the southern hemisphere. So, SLR can only give terrestrial reference frames (TRFs) at large spatial (a few thousands of kilometers) and temporal (not below 7 days) scales. Combining SLR with other techniques such as GPS and Doppler orbitography and radiopositioning integrated by satellite (DORIS) improves the geographic distribution of

<sup>1</sup>Institut Géographique National, Marne-la-Vallée, France.

<sup>2</sup>Observatoire de la Côte d'Azur, Grasse, France.

<sup>3</sup>Observatoire Midi-Pyrénées, Toulouse, France.

<sup>4</sup>Noveltis, Toulouse, France.

<sup>5</sup>Collecte Localisation Satellites, Toulouse, France.

<sup>6</sup>Observatoire de Paris, Paris, France.

stations in the global network and, for collocated sites, the temporal distribution of measurements.

[4] The present approach consists in directly combining geodetic products. As an example, the ITRF computation is based on individual sets of mean positions and velocities of ground stations [Altamimi *et al.*, 2002a]. EOPC04 time series are derived from individual EOP time series [Gambis, 2004]. Indeed, these series are computed with VLBI measurements and satellite technique measurements (GPS, SLR, and DORIS). VLBI provides absolute but sparse reference for the determination of universal time (*UT1*). Satellite techniques provide the short-period variations of this quantity (and, more particularly, its time derivative, length of day (LOD)) and pole coordinates  $x_p$  and  $y_p$ . Producing EOP time series consists in combining the solutions computed by analysis centers for each of these different techniques. Several sources of inaccuracy can alter results of such combinations.

[5] First of all, individual EOP time series may contain systematic errors. The present combination process takes these heterogeneities into account by estimating and removing linear trends [Gambis, 2004]. Other types of systematic error can thus alter results.

[6] Second, the diversity of software (algorithms, constants, and models) and strategies developed and used by analysis centers can generate inconsistencies between individual time series. Even if these inconsistencies should be reduced thanks to the use of IERS conventions [e.g., McCarthy and Petit, 2004], subtle differences may still lead to systematic effects.

[7] Furthermore, space-geodetic techniques do not have networks of the same quality. SLR and VLBI networks are poorly distributed in the southern hemisphere. Consequently, subnetwork effects can cause additional inconsistencies.

[8] Finally, the different products of IERS (ITRF, ICRF, and EOPs) are still computed independently; this inevitably leads to inconsistencies between them.

[9] In order to eliminate possible inconsistencies in solutions produced by these various techniques, we propose to combine VLBI, SLR, GPS, and DORIS techniques at the measurement level. Theoretically, this approach is the most satisfactory as it is closer to measurements. Furthermore, by using the same software to carry out the computations, we guarantee that any inaccuracy is identically shared by all the involved techniques. This kind of combination has already been investigated in the recent past and has been applied to VLBI sessions [Andersen, 2000] and to several techniques albeit over a shorter period of time (3 months) with a single estimation of station positions [Yaya, 2002].

[10] Our combination, directly based on measurements, has many advantages. First, observations for all techniques are processed with the same software (GINS/DYNAMO). They are thus processed with the same fundamental constants, the same physical models, and the same a priori values for parameters. This avoids systematic differences due to heterogeneous computational frameworks.

[11] During our combination process, we can still estimate parameters linked to individual techniques (range biases for SLR, clock parameters for VLBI, etc.) and, consequently, individual computations should still be optimal.

[12] Our combination involves independent and complementary information on common parameters. Regarding

EOPs, it must directly provide *UT1* with a regular sampling without any long-term drift. Indeed, only VLBI can really give *UT1*; all satellite techniques are by definition limited by correlations with the longitudes of the ascending nodes of the orbits. With regard to this parameter, the observational level can then be used to combine the partial derivatives of all these techniques. As a result, values estimated by VLBI can thus be interpolated through satellite techniques by reducing correlations.

[13] Our combination is clearly a first step toward an “ideal” combination at the measurement level. Indeed, theoretically speaking, such an ideal combination at the measurement level should have major advantages. First of all, radio wave techniques (GPS, DORIS, and VLBI) are still limited by atmospheric propagation. The SLR technique is not so much affected by this phenomenon. A combination could thus take advantage of the exact information provided by SLR to improve results for GPS, DORIS, and VLBI in collocated sites, by estimating common atmospheric delays, for instance.

[14] Another form of collocation could be generated by satellite orbits. Indeed, some satellites (Jason-1 for instance) are equipped to be tracked by several observational techniques. So, such an approach could also link these different techniques by this kind of spatial tie.

[15] Moreover, this kind of combination should reveal systematic differences between techniques and reduce them in order to provide EOP and station position estimations in a unified global combined TRF. This approach clearly resolves geometric problems for SLR and VLBI. Furthermore, it could lead to a validation of local ties in IERS geodetic sites. Also, these local ties could be used as complementary information during the combination process. In addition, satellite techniques can monitor geocenter motion (with different levels of accuracy). Such a combination at the observational level could also give the opportunity to estimate a combined geocenter motion. It would provide a supplementary link between SLR, GPS, and DORIS.

[16] Finally, such a combination, carried out at the measurement level, should generate all geodetic products (CRFs, TRFs, EOPs, and Earth gravity field).

[17] It is obvious that such an ambitious computation is still utopic as the problems involved are numerous and quite arduous. However, such a combination is clearly the goal to reach in the future. To this end, we are developing a new multitechnique analysis package, but it has not yet worked as well for each technique as specialist software (especially for GPS and VLBI) and the model used has not yet been optimized to carry out an optimal combination at the observational level. So, as a first computation, we have carried out a more reasonable and simple combination. Indeed, we have not considered atmospheric delays as common parameters between techniques: the GINS/DYNAMO software has not yet been upgraded to consider atmospheric delays as links between geodetic techniques. We have limited our efforts to terrestrial links and, more particularly, to EOPs ( $x_p$ ,  $y_p$ , and *UT1*). We have not used local ties between instruments in collocated sites. The reason is the problem of the heterogeneity between the terrestrial reference frames of each technique inside the combination. This problem is exhaustively discussed in section 5. Finally, considering our recent expe-

**Table 1.** Physical Models Used for the Orbit Computations

Type	Description
Earth gravity field	GRIM5_C1 [Gruber et al., 2000]
Atmospheric density	DTM94 [Berger et al., 1998]
Planetary ephemerides	DE403 [Standish et al., 1995]
<i>Earth time varying gravity field</i>	
Solid Earth tides	Model in McCarthy and Petit [2004]
Solid Earth pole tide	Model in McCarthy and Petit [2004]
Oceanic tides	FES2002 [Le Provost, 2002]
Atmospheric pressure	ECMWF <a href="http://www.ecmwf.int/">http://www.ecmwf.int/</a>

rience for GPS and VLBI computations with GINS software, we have decided to keep only EOPs and station positions as parameters worthy of interest.

[18] So, this first combination carried out at the measurement level (more rigorously at the normal system level, in fact) aims to (1) prove that combining the partial derivatives of the four techniques involved with respect to  $UT1$  can lead to an absolute universal time with the density of GPS solutions; (2) design a methodology of combination which can be used as a starting point by other groups in the world; (3) produce a concise but precise review of what can be expected from such a combination at the measurement level; (4) highlight some important problems and present some clear and precise prospects to take these critical aspects into account in the near future.

[19] In this methodological paper we describe the project of combination and, more particularly, the software and the models used as well as the individual computations for each technique. We then detail the method of combination and analyze the results obtained for EOPs. Finally, we explore ways to take advantage of such a combination to estimate not only EOPs but also homogeneous global TRFs produced weekly.

## 2. Contributions of Geodetic Techniques

### 2.1. Physical Models

[20] The test period chosen for our computations is the year 2002. More precisely, this period begins on 30 December 2001, 00 hours 00 min 00 s (modified Julian day (MJD) 52 273) and ends on 4 January 2003, 23 hours 59 min 59 s (MJD 52 646). Indeed, the station positions are estimated every GPS week (each GPS week begins on Sunday, 00 hours 00 min 00 s UTC and ends on the following Saturday, 23 hours 59 min 59 s UTC). The analysis is limited to a core of parameters: EOPs, station positions, and range biases for SLR. Other parameters like orbital coefficients or atmospheric delays, used for our computations, are previously reduced in the normal systems.

[21] The GINS/DYNAMO software was developed in the early 1970s by the Centre National d'Études Spatiales (CNES)/Observatoire Midi-Pyrénées (OMP). This software has been provided to several research groups in the framework of the Groupe de Recherche en Géodésie Spatiale (GRGS) (CNES/OMP, Noveltis, Collecte Localisation Satellite (CLS), Observatoire de la Côte d'Azur (OCA)/GEMINI, and Paris' Observatory).

[22] The physical models for the orbit computations and for the a priori variations of EOPs and station positions are described in Tables 1, 2, and 3 respectively.

**Table 2.** Physical Models Used for the EOPs

Type	Description
A priori time series	EOPC04 [Gambis, 2004]
Quasi-diurnal variations	Model of McCarthy and Petit [2004]
Greenwich Sidereal Time	Model [Aoki et al., 1982]
Precession	Model [Lieske et al., 1977]
Nutation	Model of McCarthy [1996]

[23] Regarding the global network of ground instruments, not all stations used for the computations are present in ITRF2000. Indeed, the positions of 28 DORIS beacons have previously been computed in the ITRF2000 reference frame. The eccentricities are taken equal to the values in ITRF2000 for SLR and VLBI; they are equal to zero for DORIS. Regarding GPS, these eccentricities are taken from the daily revised SINEX file `igs.snz` available at `ftp://igs.csb.jpl.nasa.gov/igs/scb/station/general`. This file also provides the phase center corrections for GPS. Regarding the DORIS technique, these corrections are 487 mm for the positioning beacons and 510 mm for the orbitography beacons.

[24] Regarding EOPs, the a priori time series are official EOPC04 time series. For each measurement, these time series are interpolated between the tabulated epoch and the considered measurement epoch with a four-point lagrangian polynomial interpolation. Regarding the interpolation of  $UT1$  time series, we do not use the model of zonal tides [Yoder et al., 1981].

[25] In order to make our results comparable to those produced by international analysis centers, we estimated EOPs ( $x_p$ ,  $y_p$ , and  $UT1$ ; the EOP rates were not computed) each day at noon. Moreover, in order to find possible evidence of quasi-diurnal residual signals, we also computed combined EOP time series with a 6-hour sampling. We implicitly consider here that these 6-hour EOP offsets are computed with respect to the EOPC04 time series with a 6-hour sampling.

[26] Equations (1) show the mathematical models used for EOPs and station positions at a given time  $t$ . The estimated parameters are the  $\delta EOP$  and  $\delta X_i$  offsets with respect to the models mentioned in Table 2 and Table 3. In order to get a satisfactory distribution of measurements, these offsets are supposed constant over a given period of time: over 6 hours or 1 day for EOPs and over 1 week for station positions. EOP  $\delta EOP$  offsets as well as estimated  $\delta X_i$  geocentric position offsets must reflect not only deficiencies in the a priori models used but also unknown

**Table 3.** Physical Models Used for the Station Positions

Type	Description
A priori reference frame	ITRF2000 [Altamimi et al., 2002a]
Celestial reference frame <sup>a</sup>	ICRF [Arias et al., 1995]
Solid Earth tides	Model of McCarthy and Petit [2004]
Solid Earth pole tide	Model [Wahr, 1985]
Oceanic loading <sup>b</sup>	Computed with FES2002
Atmospheric loading <sup>c</sup>	Computed with field of ECMWF

<sup>a</sup>The celestial reference frame is only used for VLBI.

<sup>b</sup>We only use tidal components.

<sup>c</sup>We only use nontidal components.

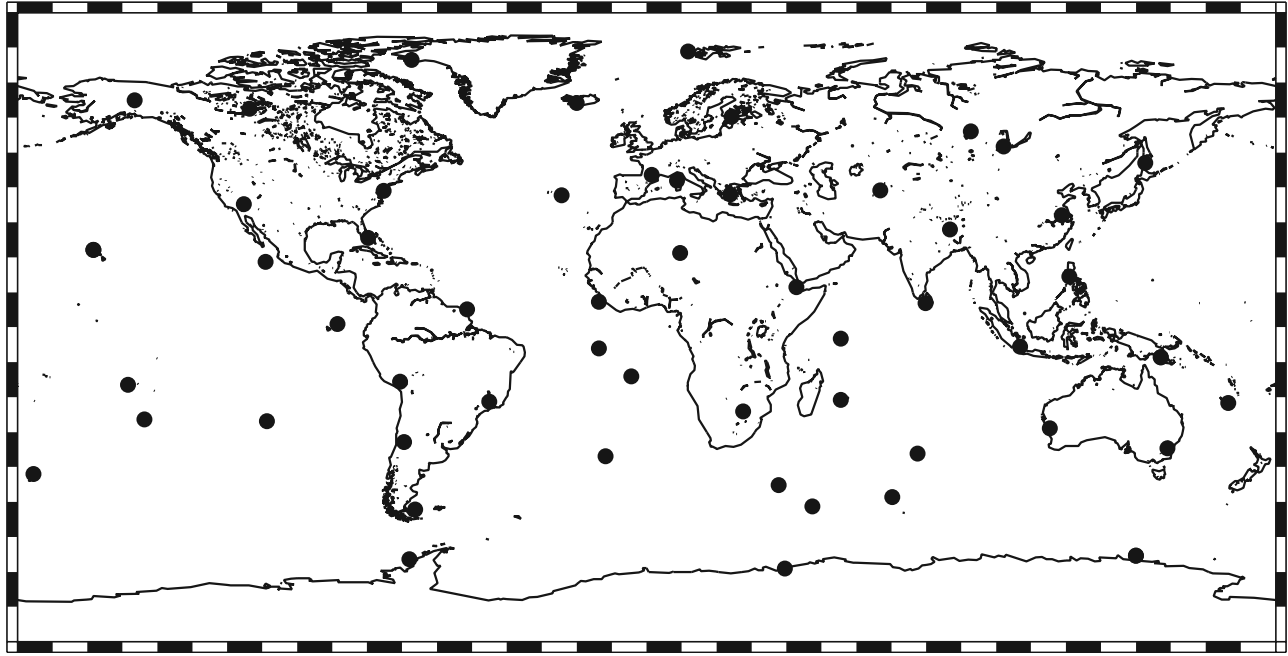


**Figure 1.** Doppler orbitography and radiopositioning integrated by satellite (DORIS) beacon network used for the computations.

signals or even artificial signals induced by the computation methods.

$$\begin{aligned}
 EOP(t) &= EOP^{a\text{ priori}}(t) + \delta EOP(t) \\
 EOP^{a\text{ priori}}(t) &= EOP^{EOPC04}(t) + EOP^{q\text{-diur.}}(t) \\
 X_i(t) &= X_i^{a\text{ priori}}(t) + \delta X_i \\
 X_i^{a\text{ priori}}(t) &= X_i^{ITRF2000}(t_0) \\
 &\quad + \dot{X}_i^{ITRF2000}(t_0)(t - t_0) \\
 &\quad + X_i^{Earth\text{ tid.}}(t) + X_i^{pol.\text{ tid.}}(t) + X_i^{load.}(t)
 \end{aligned} \quad (1)$$

## 2.2. DORIS

[27] The 3.5-day orbital arcs are computed for five satellites: Satellite Pour l'Observation de la Terre (SPOT) 2, 4, and 5, ocean Topography Experiment (TOPEX/Poséidon) and Environmental Satellite (ENVISAT). This length of arc is in fact variable (between 1 and 3.5 days) to take orbit correction maneuvers and data gaps into account. Drag coefficients, solar pressure coefficients, tropospheric zenithal delays, frequency biases, and empirical parameters [Crétau et al., 1994] are estimated during the orbit processing. The estimation of tropospheric zenithal delays is based on the CNET mapping function [Baby et al., 1988]. The network of ground beacons used for DORIS computations is shown in Figure 1. The data from a total number of 58 beacons are processed and the data from a mean number of 47 beacons are used every week. Measurements for each satellite alone do not necessarily cover the whole test period as shown in Table 4. However, by gathering the weekly normal matrices for all the satellites, we generated 53 weekly normal matrices covering the test period.

[28] Table 5 shows the amounts of data (mean values are given for 3.5-day orbital arcs) used for the DORIS

computations and the mean weighted RMS values of the orbital residuals. These RMS values indicate a good consistency between the orbital arcs of the three SPOT satellites and TOPEX/Poséidon. For ENVISAT, the RMS values are a little bit larger. It must be noticed that these DORIS computations are carried out by LEGOS/CLS, an official International DORIS Service (IDS) analysis center.

## 2.3. GPS

[29] Two-day orbital arcs are computed for the satellites of the GPS constellation. We process undifferentiated (phase and pseudo-range) iono-free measurements at a sampling rate of 900 s. The atmospheric drag is ignored. We consider phase ambiguities as real-valued parameters. The elevation cutoff angle is 15 degrees for phase and range data. Clock parameters are adjusted as independent parameters for each epoch of 900 s and for each station and each GPS satellite (except for one station which is kept as reference). A tropospheric vertical bias is estimated for each station every 3 hours using the CNET mapping function [Baby et al., 1988]. The solar pressure force is modelled by using empirical Bar-Sever's model [Bar-Sever and Kuang, 2003] and we compute a bias in the Y direction and a scale factor per day on the pressure force for each GPS satellite. No pseudo-range biases are applied. The a priori standard deviation values are 1 m (1 cm) for range (phase) measurements.

**Table 4.** Distribution of the DORIS Measurements in Time

Satellite	Data Beginning	Data Ending
SPOT 2	2001.12.30	2003.01.04
SPOT 4	2001.12.30	2003.01.04
SPOT 5	2002.06.16	2003.01.04
TOPEX/Poséidon	2001.12.30	2003.01.04
ENVISAT	2002.07.21	2003.01.04

**Table 5.** Amounts of Data Used (Total Amount/Mean Amount Per 3.5-Day Orbital Arc) and Mean Weighted RMS Values of the Residuals for the DORIS Orbit Computations

Satellite	Data Used	RMS Values
SPOT 2	14 273/135	0.45 mm/s
SPOT 4	14 719/140	0.45 mm/s
SPOT 5	20 929/197	0.41 mm/s
TOPEX/Poseidon	18 763/177	0.44 mm/s
ENVISAT	11 174/105	0.53 mm/s
Total amount	79 858/753	

[30] The ground network of receivers used for the GPS computations (Figure 2) does not encompass all the existing GPS receivers; it is clearly a reduced network. Indeed, this network results from a compromise between the processing capacities of GINS software (data volume, type of receivers manageable by the software, etc.) and the quality of the computed orbits: the receivers which give large orbit residuals are eliminated. For instance, KOUR is not manageable by our computation chains, and so this station appears only once during the whole year 2002. However, we try to always keep a satisfactory distribution of the receivers for the obtained global network. The data from a total number of 72 receivers are processed and the data from a mean number of 59 receivers are used every week.

[31] The amounts of data (mean values are given for 2-day orbital arcs) used for the GPS computations and the mean weighted RMS values of the orbital residuals are shown in Table 6. Furthermore, comparisons of our orbits with respect to the official International GNSS Service (IGS) combined orbit show three-dimensional RMS values of differences 2.5 to 3 times larger than those obtained with the orbits of IGS analysis centers. This comparison shows

that our GPS computations are not yet at the level of the best international GPS data processing.

## 2.4. SLR

[32] The two geodetic Laser Geodynamics Satellites (LAGEOS) are used for the SLR computations. Nine-day orbital arcs are computed for these satellites, but only the 7 central days of these arcs are kept for parameter estimation. Indeed, remaining orbital errors have a stronger value at the beginning and at the end of individual orbital arcs. In order to significantly reduce these orbital errors, we also compute empirical parameters deduced from Hill's theory [Crétau et al., 1994] for the three directions (radial, along-track, and across-track). The tropospheric correction is based on the model in the work of Marini and Murray [1973]. Furthermore, we have developed and used a new way of computing range biases. Indeed, these biases are largely correlated with station position vertical components. As a result, if they are not estimated, we can damage the estimations of these vertical components and, as a consequence, the scale of the underlying TRF. To avoid this problem, we use our temporal decorrelation method [Exertier et al., 2004] consisting in estimating range biases per satellite over a long period together with all the other parameters.

[33] The SLR ground station network used is shown in Figure 3. This network is in fact a dynamic network. Indeed, all stations in this network do not necessarily provide the same amount of data on the two LAGEOS satellites every week. The stations for which the total amount of data on both LAGEOS satellites do not exceed 20 normal points on a given week are removed from computations. Including these stations in the network can induce numerical problems in the parameter estimation (see section 5.2). The data from a total number of 29 stations are processed and the data from a mean number of 17 stations are used every week. The amounts of data (mean values are given for the 7-day

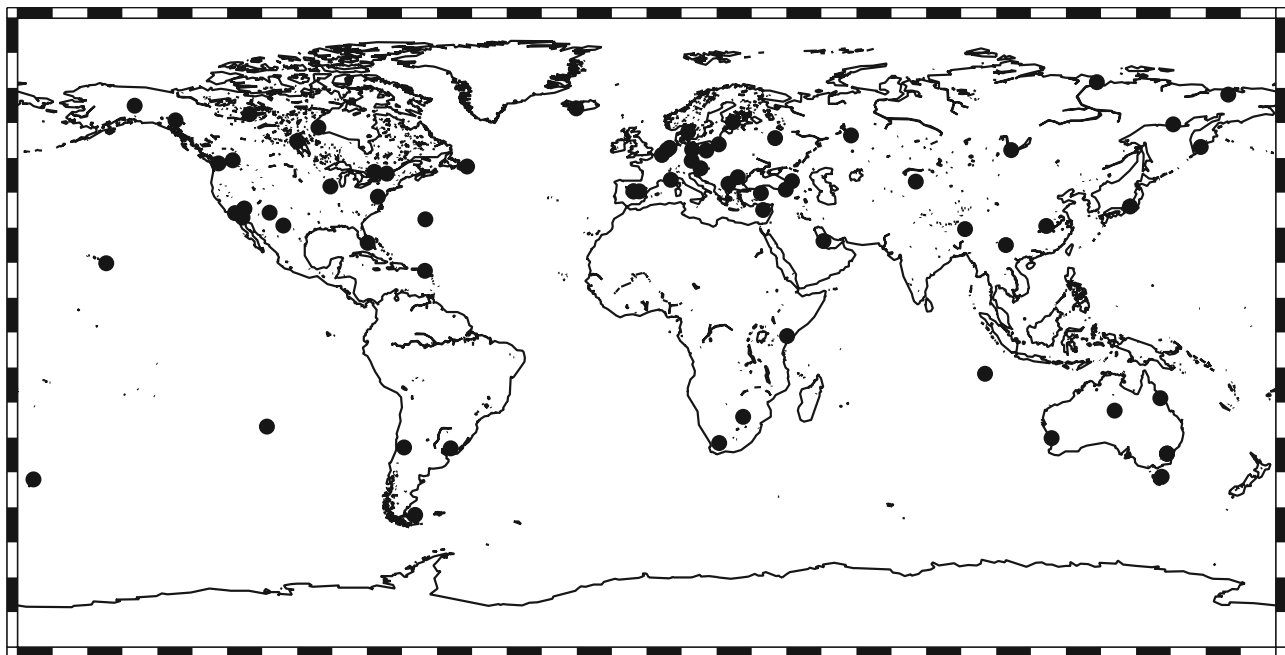


**Figure 2.** GPS receiver network used for the computations.

**Table 6.** Amounts of Data Used (Total Amount/Mean Amount Per 2-Day Orbital Arc) and Mean Weighted RMS Values of the Residuals for the GPS Orbit Computations

Measurement	Data Used	RMS Values
Pseudo-range	10 132 187/54 621	36.3 cm
Phase	10 132 187/54 621	5.7 mm
Total amount	20 264 374/109 242	.

orbital arcs actually kept) used for the SLR computations are shown in Table 7. This table also shows the mean weighted RMS values of the orbital residuals. These centimeter RMS values are satisfactory. Moreover, comparisons of our orbits with orbits computed by an official International Laser Ranging Service (ILRS) analysis center reveal three-dimensional RMS values of differences at the level of 2–3 cm.

## 2.5. VLBI

[34] Regarding the VLBI computations, all relativistic effects are rightly handled in barycentric timescale and frame in agreement with the recommended conventions [McCarthy and Petit, 2004]. Indeed, these relativistic effects are taken into account in the transformation between the geocentric and the barycentric frames (Lorentz’s transformation). They are also applied to model the effect of radio wave propagation in solar system (the effects of the Sun, the Moon, and the Earth are considered). We consider instrumental and atmospheric delays. Only the group delays are used and the considered tropospheric model is the model in the work of Niell [1996]. Moreover, zenithal delays are estimated twice hourly.

[35] We use four types of data from the International VLBI Service (IVS) programs: IVS-R1 (database code (DBC) XA, named “sessions A” in the following), IVS-R4 (DBC XE, called “sessions E” in the following), JARE project (DBC

XF, named “sessions F” in the following), and, finally, intensive sessions for *UT1* (the so-called “sessions U”). The IVS-R1 and IVS-R4 programs aim to provide EOP estimations twice a week. The Japanese Antarctic Research Expedition (JARE) project is intimately linked to the Syowa Antarctica and OHIGGINS programs. This latter aims to detect tectonic motions and to improve the TRF in the southern hemisphere. Finally, intensive sessions are reserved for *UT1* computation. They use a unique east-west baseline (Kokee, USA to Wettzell, Germany). For more details on these programs, please consult the Web site <http://ivscc.gsfc.nasa.gov/program/descrip2002.html>. By combining these different sessions, we aim to take advantage of all existing VLBI measurements to better estimate EOPs. This combination is fully described by Coulot [2005]. Although we work with individual VLBI sessions which can be sparsely located in time, we add them together in order to obtain weekly normal matrices. This mixing is consistent with the other geodetic techniques and can especially be used to compute the TRF linked to this technique every week. It can seem odd to use the VLBI intensive sessions: the geometry of the data involved is indeed highly biased due to the long east-west baseline with limited mutual visibility. In fact, there is no reason to exclude the session U data in the computations if all the session types are combined together. Indeed, in this case, the geometry is satisfactorily completed by the other sessions for which the same antennae have been used. Furthermore, numerical tests have proved that the combined *UT1* results were damaged if the session U data were not included in the computation process [Coulot, 2005]. Figure 4 illustrates the ground network of VLBI antennae used for the computations. This network is dynamic as it depends on the sessions used for a given week. The data from a total number of 21 antennae are processed and the data from a mean number of 6 antennae are used every week. Indeed, sessions A can

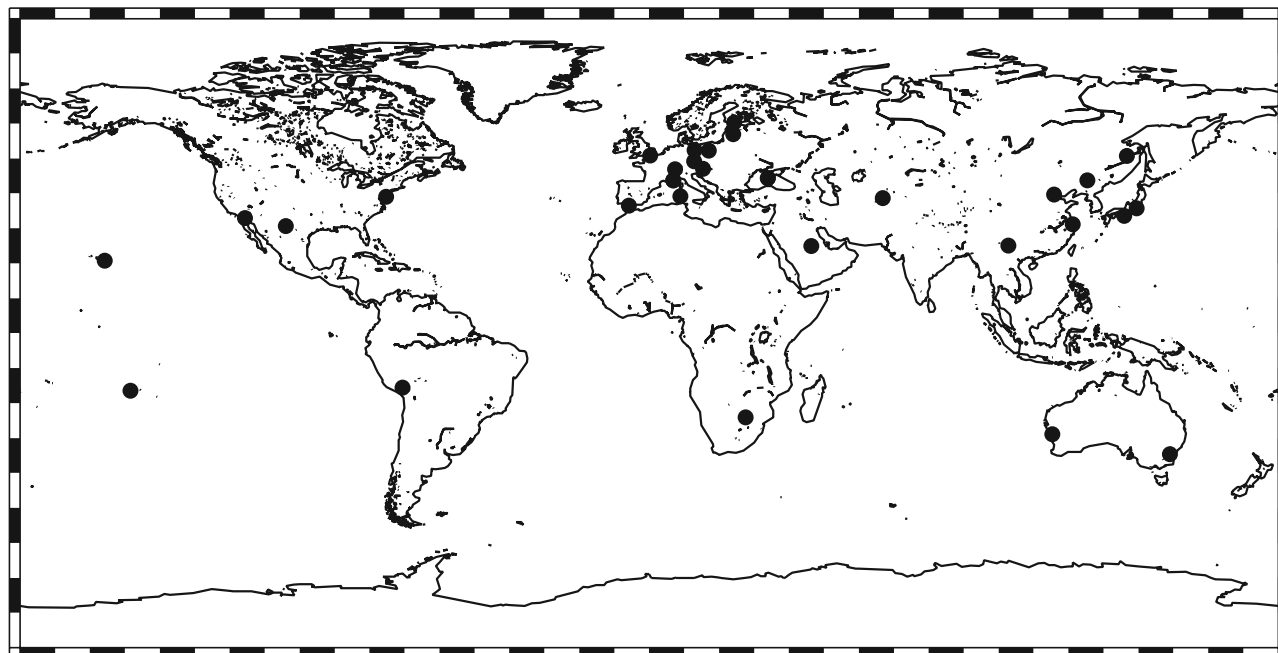


**Figure 3.** Satellite laser ranging (SLR) station network used for the computations.

**Table 7.** Amounts of Data Used (Total Amount/Mean Amount Per 7-Day Orbital Arc) and Mean Weighted RMS Values of the Residuals for the SLR Orbit Computations

Satellite	Data Used	RMS Values
LAGEOS-1	64 342/1 214	1.23 cm
LAGEOS-2	58 035/1 095	1.00 cm
Total amount	122 377/2 309	.

involve 6–8 antennae, sessions E can involve 6–8 antennae, sessions F can require up to 6 antennae, and sessions U use only 2 antennae. The amounts of data (mean values are given with respect to the chosen weekly sampling) used for the VLBI computations and the mean weighted RMS values of the estimation residuals are shown in Table 8. The RMS values are converted into metric values in order to be comparable with those of the other techniques. The results show a global mean RMS value over all the different sessions close to 1 cm. This mean value shows that our VLBI computations are not yet at the level of the best international VLBI computation.

### 3. Combination Method

#### 3.1. Reference System Effects

[36] Inversion of normal matrices involving station position offsets can give rise to difficulties. Indeed, these normal matrices can have significant rank deficiencies. Thus their inversion is impossible without the addition of the lacking information. These rank deficiencies are directly linked to deficiencies in the definition of the underlying TRFs; all space-geodetic techniques are not sensitive to all degrees of freedom of a TRF in space. The reference system effect is a criterion identifying such badly defined degrees through the variance matrix of station position solutions computed for a geodetic technique with a given analysis strategy [Sillard and Boucher, 2001]. When these badly defined degrees of

freedom are identified, minimum constraints can be added to the normal matrices in order to provide the necessary information and no more [Altamimi et al., 2002b]. The reference system effect criterion has been developed, tested, and validated for variance matrices of station positions [Sillard and Boucher, 2001]. However, all space-geodetic computations now involve not only station positions but also EOPs. These EOPs provide the orientation of their underlying TRF. For this reason, we decided to generalize reference system effect to EOPs. In the context of the estimation of daily EOPs over a given week (presently the most usual configuration of space-geodetic computations), we can write the transformation between EOPs linked to two TRFs 1 and 2:

$$EOP^2 = EOP^1 + B \cdot \begin{pmatrix} R_X \\ R_Y \\ R_Z \end{pmatrix} = EOP^1 + B \cdot \rho \quad (2)$$

with [cf. Zhu and Mueller, 1983]

$$EOP^i = \begin{pmatrix} x_p^i(t_1) \\ \vdots \\ x_p^i(t_7) \\ y_p^i(t_1) \\ \vdots \\ y_p^i(t_7) \\ UT1^i(t_1) \\ \vdots \\ UT1^i(t_7) \end{pmatrix} \text{ and } B = \begin{pmatrix} 0 & -1 & 0 \\ \vdots & \vdots & \vdots \\ 0 & -1 & 0 \\ -1 & 0 & 0 \\ \vdots & \vdots & \vdots \\ -1 & 0 & 0 \\ 0 & 0 & \frac{1}{f} \\ \vdots & \vdots & \vdots \\ 0 & 0 & \frac{1}{f} \end{pmatrix} \quad (3)$$

where  $f = 1.002737909350795$  is the ratio between sidereal and universal times [Aoki et al., 1982]. The entire development used to derive the reference system effect theory [cf. Sillard and Boucher, 2001] can be transposed to EOPs, the starting point being the previous relations (2) and (3). Here is the result. Considering  $\Lambda$  the variance matrix of

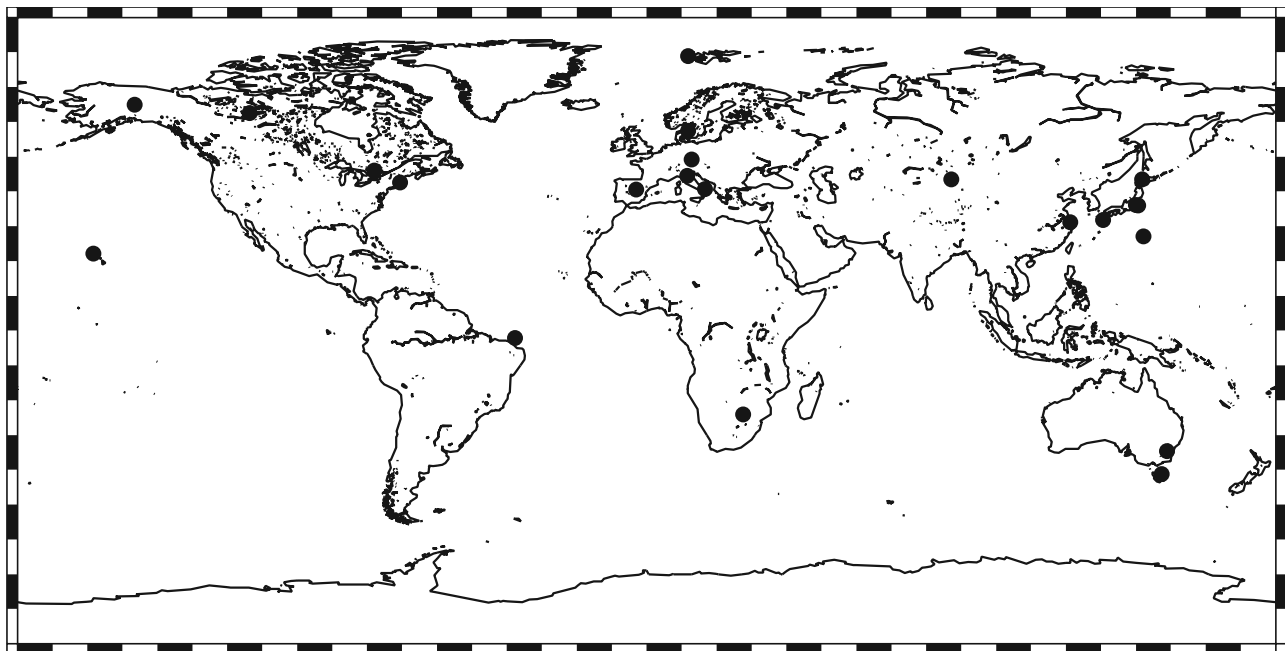


**Figure 4.** Very long baseline interferometry (VLBI) antenna network used for the computations.

**Table 8.** Amounts of Data Used (Total Amount/Mean Amount Per Week) and Mean Weighted RMS Values of the Residuals for the VLBI Computations

Session	Data Used <sup>a</sup>	RMS Values
Session A	15 858/1 982	1.41 cm
Session E	43 208/1 080	1.26 cm
Session F	6 055/1 211	2.22 cm
Session U	2 681/51	0.65 cm
Total amount	67 802/1 279	-

<sup>a</sup>For sessions A we have 8 weeks of data, 40 weeks for sessions E, 5 weeks for sessions F, and 53 weeks (so the whole year 2002) for sessions U.

a given EOP set,  $\Lambda$  can be decomposed in a unique way as follows:

$$\left\{ \begin{array}{l} \text{variance matrix} \\ \Lambda \end{array} \right. = \left. \begin{array}{l} \text{internal noise} \\ \Lambda_0 \end{array} \right. + \left. \begin{array}{l} \text{ref. sys. effect} \\ B \cdot \Lambda_\rho \cdot B^T \end{array} \right. \quad (4)$$

$\Lambda_0 = Q_{\Lambda^{-1}} \cdot \Lambda \cdot Q_{\Lambda^{-1}}^T$  and  $\Lambda_\rho = (B^T \cdot \Lambda^{-1} \cdot B)^{-1}$

where  $Q_{\Lambda^{-1}} = I - B(B^T \Lambda^{-1} B)^{-1} B^T \Lambda^{-1}$ . Numerical examples of such reference system effects are given in sections 4 and 5.

**3.2. Computational Scheme**

[37] The scheme in Figure 5 describes in details all the computations carried out during this project. First of all, the GINS software, on the basis of the measurements and the physical models described in section 2.1 (Table 1, Table 2, and Table 3), produces weekly individual normal systems related to EOPs, station positions, and range biases for the SLR technique. These weekly individual normal systems generated for DORIS, GPS, SLR, and VLBI are the starting points of all the computations. In order to compare our results with the international analysis center solutions (section 4.1), we carry out individual computations. Moreover, the comparison between these individual solutions and the solutions produced with the combination of the four techniques is a direct internal validation of our method

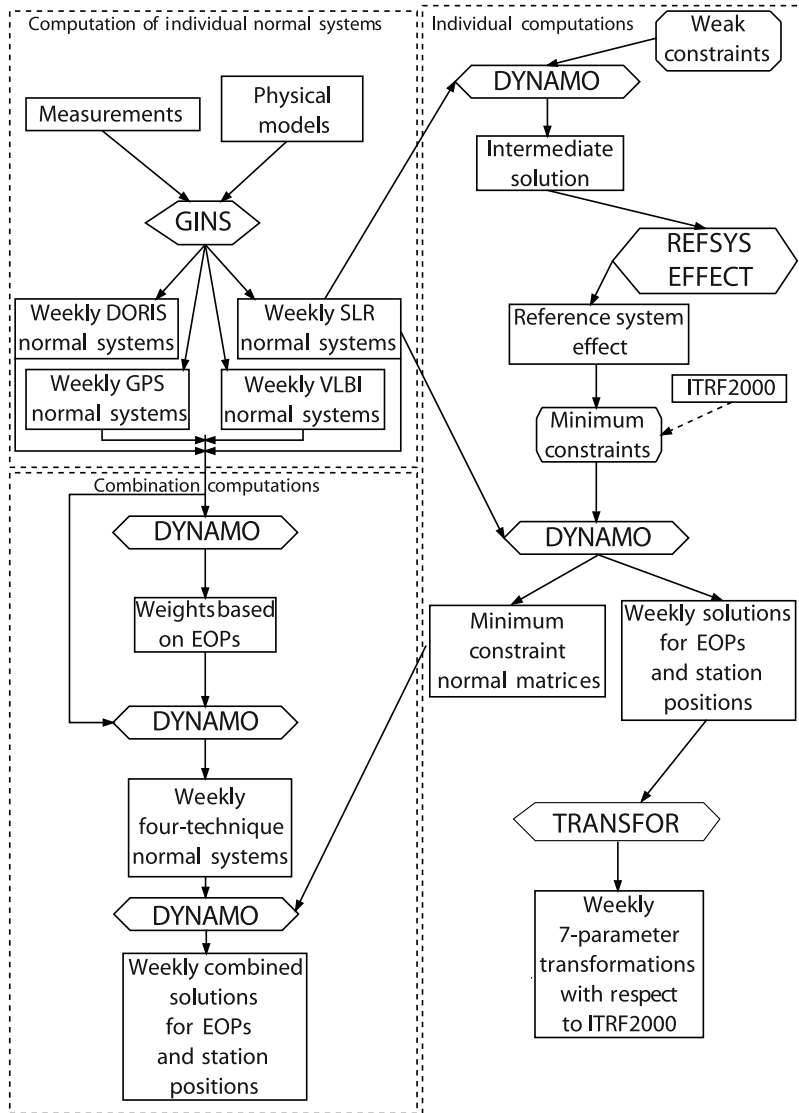


**Figure 5.** Methods used to compute the individual normal systems and, based on these systems, the individual and combined solutions.

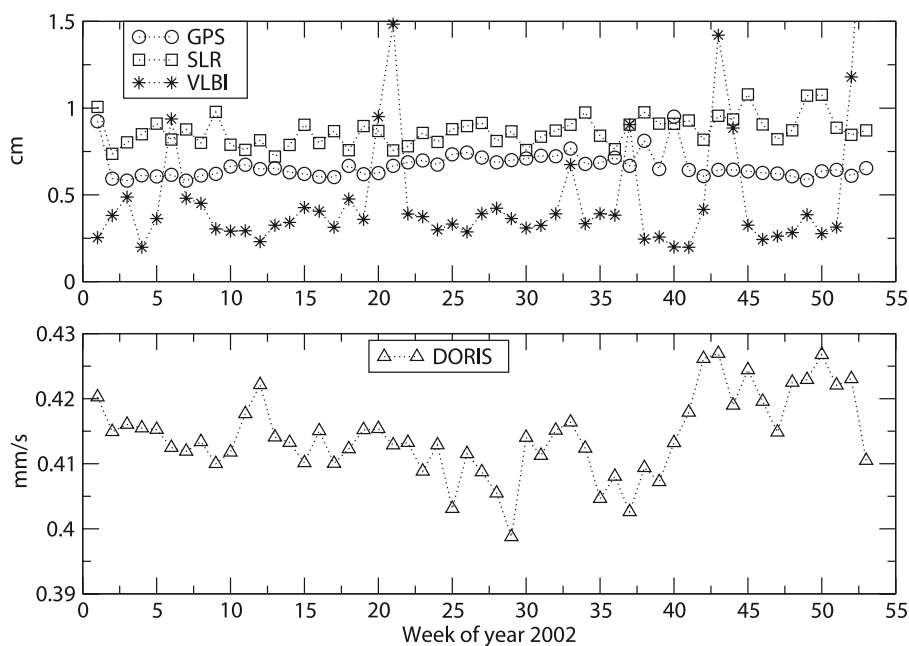


**Figure 6.** Relative weights of the individual techniques in the combination. The weights are translated into a priori standard deviation values of the measurements in centimeters for GPS, SLR, and VLBI and in millimeters per second for DORIS.

(section 4.2). For a given technique, an intermediate solution is computed each week with the addition of weak constraints (1 m for station positions and equivalent values for EOPs). On the basis of these weekly intermediate solutions, we carry out studies of the reference system effects (software “REFSYS EFFECT” in Figure 5). Deficiencies in definition of the weekly underlying TRFs being identified, minimum constraints are added to the normal systems. We then solve these systems to compute the weekly solutions (with a daily sampling for EOPs) in the TRF linked to the technique. These minimum constraints are applied with respect to ITRF2000. On the basis of the station position solutions, the software “TRANSFOR” computes the weekly seven-parameter transformations between our weekly individual TRF solutions and ITRF2000. Each week, the optimal values of the relative weights are computed for the individual techniques through their combination. These weights are based on the EOP statistics (see next section 3.3). Then, these weights are used to generate the weekly four-technique normal systems mixing the measurements and the partial derivatives of all the techniques. By applying minimum constraints per technique, these weekly combined normal systems are used to compute the combined EOPs (with 1-day or 6-hour samplings) and the weekly station positions. The use of minimum constraints in the framework of the combination computations is discussed in section 5.

### 3.3. Weighting Technique

[38] In order to take the best advantage of each technique for EOP computation, the weekly individual normal systems per technique are weighted by using an optimal variance component estimation method [Sahin *et al.*, 1992]. Computing these relative weights requires common parameters between techniques. With regard to our estimation model, only EOPs are real common parameters. Fur-

thermore, satellite techniques can provide these EOPs with a regular sampling, but VLBI can not. Consequently, the common parameters used are in fact the EOPs at the times provided by the natural sampling of the VLBI measurements. It would be more rigorous to use all common parameters between techniques to compute optimal weights: in other words, to use not only EOPs but also positions of collocated instruments as it is done for the ITRF computation [Altamimi *et al.*, 2002a]. However, the heterogeneity of the individual technique reference frames inside the combination (see section 5) prevented us from using local ties and, as a consequence, considering collocated station positions for the estimation of the optimal weights. Figure 6 shows the weekly computed weights for the four techniques. Measurements of techniques are a priori weighted. The weights of these techniques in the combination are the products of the variance components computed with Helmert’s method and the a priori weight matrices [cf. Sahin *et al.*, 1992]. To better study the actual weights assigned to the individual techniques in the combination, we translate the variance scale factors into a priori standard deviation values of measurements. Table 9 shows the mean values of these a priori standard deviation values for each technique alone and inside the combination.

[39] The weights are very stable for the DORIS, GPS, and SLR techniques. Indeed, the RMS values of the a priori standard deviation values are 0.006 mm/s for DORIS, 0.07 cm for GPS, and 0.08 cm for SLR. For VLBI, the RMS value is 0.41 cm. Indeed, Figure 6 shows values larger than 0.5 cm, thus less important weights, for 9 weeks in the year 2002 (weeks 6, 20, 21, 33, 37, 43, 44, 52, 53). For all these weeks (except for the week 37), only the measurements of the sessions U were used to compute the VLBI normal system. These sessions can not provide all EOPs but only *UT1* (see section 2.5). The weighting of

**Table 9.** Mean A Priori Standard Deviation Values of the Measurements of Each Technique Individually and in the Combination

Technique	Individually	In the Combination
DORIS, mm/s	0.57	0.41
GPS, cm	1.50	0.67
SLR, cm	1.11	0.87
VLBI, cm <sup>a</sup>	0.54	0.49

<sup>a</sup>In order to make them comparable with other results, the values for VLBI are converted into centimeters.

the techniques is based on all the EOPs at the times provided by VLBI. This is the reason why, for these particular weeks, VLBI is less weighted.

[40] Table 9 shows that the most weighted technique is GPS. Indeed, the a priori standard deviation values of the measurements are divided by about 2 in the combination for this technique. Furthermore, the standard deviation values for VLBI are small and at the level of those obtained for GPS. This technique does not have a negligible weight in the combination even if the gain between standard deviation values is only 1.1; the gain is the ratio between the mean a

priori standard deviation values of measurements for the technique alone and inside the combination. This gain is 1.3 for SLR for which the standard deviation values are higher than GPS and VLBI values. So, this technique is less weighted in the combination. Finally, the gain of 1.4 obtained for DORIS is comparable to the SLR gain. The variance scale factors for these techniques are at the same level. Although the values are not necessarily easy to interpret for DORIS, the individual results described in section 4 show that this technique is certainly less weighted than the three others.

## 4. Results for EOPs

### 4.1. Solutions Per Technique

[41] We are fully conscious that our GPS and VLBI computations have not yet been optimized, compared to computations carried out by international analysis centers. Nevertheless, in order to be rigorous and to make possible for readers to assess the quality of our individual computations, our individual daily EOP solutions are compared here with the solutions of the international analysis centers which provide the operational EOP time series used to

**Table 10.** Description of the International Analysis Center Operational EOP Time Series Used to Produce the Combined Series C04 of the IERS EOP Product Center, the Official Combined EOP Solutions From the International Services (IGS, IVS, and ILRS), and Our Individual EOP Solutions<sup>a</sup>

Center Code	Center Name and Location	$x_p$	$y_p$	$UT1$	$\dot{x}_p$	$\dot{y}_p$	$LOD$	$d\psi$	$d\epsilon$
CODE <sup>b</sup>	Bern University, Switzerland	•	•	•	•	•	•		
EMR	Energy, Mines and Resources, Canada	•	•	•	•	•	•		
ESOC	European Space Agency Operational Centre, Germany	•	•	•	•	•	•		
GFZ	GeoForschungZentrum, Germany	•	•	•	•	•	•		
JPL	Jet Propulsion Laboratory	•	•	•	•	•	•		
NOAA	National Oceanic and Atmospheric Administration, United States	•	•	•	•	•	•		
SIO	Scripps Institution of Oceanography, United States	•	•	•	•	•	•		
IGS	International GNSS Service official combined solution	•	•	•	•	•	•		
GRGS	Groupe de Recherche en Géodésie Spatiale, France	•	•	•					
AUS <sup>c</sup>	Geoscience, Australia	•	•	•				•	•
BKG	Bundesamt für Kartographie und Geodäsie, Germany	•	•	•				•	•
BKG int. <sup>d</sup>	Bundesamt für Kartographie und Geodäsie, Germany			•					
GSFC	Goddard Space Flight Center, United States	•	•	•				•	•
GSFC int.	Goddard Space Flight Center, United States			•					
IAA	Institute for Applied Astronomy, Russia	•	•	•				•	•
IAA int.	Institute for Applied Astronomy, Russia			•					
MAO	Main Astronomic Observatory, Ukraine	•	•	•				•	•
SPBU	Saint-PetersBurg University, Russia	•	•	•				•	•
SPBU int.	Saint-PetersBurg University, Russia			•					
USNO	United States Naval Observatory, United States	•	•	•				•	•
IVS	International VLBI Service official combined solution	•	•	•				•	•
GRGS	Groupe de Recherche en Géodésie Spatiale, France	•	•	•					
GRGS int.	Groupe de Recherche en Géodésie Spatiale, France			•					
CSR <sup>e</sup>	Center for Space Research, United States	•	•	•					
DUT	Delft University of Technology, Netherlands	•	•	•					
IAA	Institute for Applied Astronomy, Russia	•	•	•					
MCC	Mission Control Center, Russia	•	•	•				•	
ILRS	International Laser Ranging Service official combined solution	•	•	•				•	
GRGS	Groupe de Recherche en Géodésie Spatiale, France	•	•	•					
JPL <sup>f</sup>	Jet Propulsion Laboratory	•	•	•					
GRGS	Groupe de Recherche en Géodésie Spatiale, France	•	•	•				•	

<sup>a</sup>For each solution, the center code used in the text, the center name, and its geographical location are listed. Black disks indicate which EOPs are estimated in the considered solution.

<sup>b</sup>These nine solutions are GPS solutions.

<sup>c</sup>These fourteen solutions are VLBI solutions.

<sup>d</sup>Here “int.” corresponds to the  $UT1$  only based on the measurements from the VLBI intensive sessions U.

<sup>e</sup>These six solutions are SLR solutions.

<sup>f</sup>These two solutions are DORIS solutions.

**Table 11.** Statistics of the Differences Between the EOP Solutions Described in Table 10 and EOPC04 Time Series “sol.-C04” or the Official Combined Solution From the Corresponding International Service “sol.-offic.”<sup>a</sup>

Center Code	$x_p$ sol.- C04	$y_p$ sol.- C04	$UT1$ sol.- C04	$x_p$ sol.- offic.	$y_p$ sol.- offic.	$UT1$ sol.- offic.
CODE	-11/63	245/79	.	-5/126	10/54	.
EMR	11/77	226/73	.	34/87	8/84	.
ESOC	38/120	297/100	.	53/139	82/104	.
GFZ	-21/86	170/91	.	-2/75	-38/81	.
JPL	-21/63	227/56	.	-1/92	0/47	.
NOAA	-26/183	329/183	.	7/197	123/203	.
SIO	3/74	295/55	.	24/94	69/62	.
IGS	-28/47	223/47	.	.	.	.
GRGS	-37/102	159/101	.	-17/116	-76/123	.
AUS	-152/160	388/138	26/64	26/139	106/130	-61/227
BKG	-120/205	426/165	17/114	77/152	139/141	-92/145
BKG int.	.	.	95/182	.	.	-520/137
GSFC	-27/128	57/129	-32/130	155/124	-221/102	-109/153
GSFC int.	.	.	-22/184	.	.	-154/267
IAA	-153/162	401/139	28/94	40/125	129/108	-133/124
IAA int.	.	.	106/137	.	.	-5/326
MAO	-249/225	440/250	-28/116	-105/264	174/235	-116/166
SPBU	-61/124	118/99	-2/57	123/176	-157/171	-100/246
SPBU int.	.	.	121/152	.	.	0/261
USNO	-185/177	330/131	53/129	25/139	57/108	-1/156
IVS	-188/161	284/162	69/72	.	.	.
GRGS	-135/225	187/243	38/111	81/226	-104/258	-31/132
GRGS int.	.	.	47/137	.	.	-22/155
CSR	-1982/372	-1637/449	.	-1895/377	-1840/414	.
DUT	665/341	907/314	.	736/334	717/314	.
IAA	22/163	65/151	.	125/205	-128/192	.
MCC	-169/179	-45/172	.	-69/231	-247/225	.
ILRS	-107/168	203/175	.	.	.	.
GRGS	39/245	210/208	.	153/267	-10/229	.
JPL	251/1640	-157/828	.	.	.	.
GRGS	-416/939	-229/837	.	.	.	.

<sup>a</sup>For each parameter, the weighted mean/weighted standard deviation values are shown. Units are  $\mu\text{as}$  for  $x_p$  and  $y_p$  and  $0.1 \mu\text{s}$  for  $UT1$ .

<sup>b</sup>As these parameters do not have physical sense, we have omitted the statistics of the  $UT1$  values derived from satellite techniques.

achieve the combined C04 series of the IERS EOP Product Center. We got these solutions from the IERS EOP Product Center official Web site, <http://hpiers.obspm.fr/eop-pc/>. These operational time series and our individual EOP time series are also compared with the three international service (IGS, IVS, and ILRS; the IDS has not yet provided an official combined solution) official combined solutions. These solutions were obtained from the Crustal Dynamics Data Information System (CDDIS) Web site, <http://cddis.nasa.gov/>. All these solutions are described in Table 10 which lists the center codes used in Table 11, the center names, and geographical locations and, finally, indicates the estimated EOPs in the considered solution. Our individual solutions are named “GRGS.” Table 11 shows the statistics of all the solutions described in Table 10. More precisely, it shows the weighted mean and standard deviation values of the differences between these solutions and EOPC04 time series and the corresponding official combined solution.

#### 4.1.1. GPS Solutions

[42] Regarding GPS, the international solutions exhibit negligible biases for the  $x_p$  pole coordinate (the mean value is about  $-4 \mu\text{as}$ ) with respect to EOPC04 time series. This mean bias is still low with respect to the IGS official combined solution (the value is  $16 \mu\text{as}$ ). On the contrary, the biases with respect to EOPC04 series are significant for  $y_p$ ; the mean bias is  $256 \mu\text{as}$ . This bias between GPS solutions and EOPC04 series is well known

[Gambis, 2004]. Furthermore, this bias is present in all the GPS solutions: it thus seems to be a bias directly linked to the technique and not an artificial bias linked to the computation method. Of course, this bias disappears when the GPS solutions are compared with the IGS official combined solution (the mean value is  $36 \mu\text{as}$ ). Indeed, the IGS official combined solution has a  $223 \mu\text{as}$  bias with respect to EOPC04 series. This significant bias for  $y_p$  with respect to EOPC04 series is also present in our solution ( $159 \mu\text{as}$ , nearly half of the mean value found for the international solutions). Concerning the standard deviation values, the GPS solutions are relatively homogeneous. Indeed, the mean value is  $95 \mu\text{as}$  for  $x_p$  and  $91 \mu\text{as}$  for  $y_p$ . Results obtained for our solutions ( $102$  and  $101 \mu\text{as}$ ) are larger than these mean values. Furthermore, we can notice in Table 11 that they are almost twice of the best values obtained for the international solutions. Moreover, we must notice that all the international centers compute not only EOPs but also EOP rates; we do not compute these rates. Also, it is well known that estimating a more important number of parameters can significantly noise solutions. Finally, the values obtained with respect to the IGS official combined solution (nearly  $4 \text{ mm}$  for the two pole coordinates) are a bit large.

#### 4.1.2. VLBI Solutions

[43] For VLBI, the mean biases of the international solutions with respect to EOPC04 time series are  $-135 \mu\text{as}$  for  $x_p$ ,  $309 \mu\text{as}$  for  $y_p$ , and  $9 \text{ } 0.1 \mu\text{s}$  for  $UT1$ , respectively. The

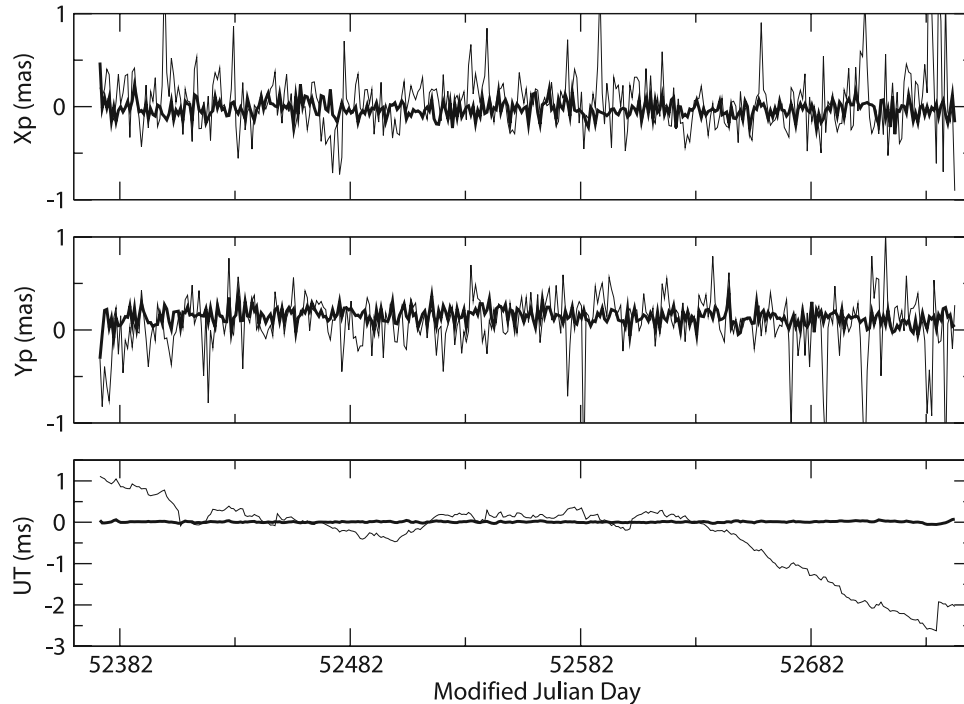


**Figure 7.** Comparison between the daily EOP offset time series produced with the SLR technique (thin curves) and with the combination of the four techniques (thick curves), respectively. Units are mas for polar motion and milliseconds for  $UT1$ .

great agreement between VLBI  $UT1$  solutions and EOPC04 solution is predictable. Indeed, only VLBI can provide absolute  $UT1$  values. On the other hand, the biases are really significant for pole coordinates. However, they are reduced when the international solutions are compared with the IVS combined solution. Indeed, the mean values are  $46 \mu\text{as}$  for  $x_p$  and  $32 \mu\text{as}$  for  $y_p$ . Regarding the weighted standard deviation values, the mean values with respect to EOPC04 time series are 143 and  $150 \mu\text{as}$  for pole coordinates and 101 and  $160 \text{ } 0.1 \mu\text{s}$  for  $UT1$  and  $UT1$  only computed with the intensive session data, respectively. These mean values are larger than GPS values. Indeed, VLBI is a little bit less sensitive to polar motion than GPS is. The values obtained for our solution for  $x_p$  and  $y_p$  with respect to EOPC04 series ( $225$  and  $243 \mu\text{as}$ ) are very large compared to the mean values obtained for the international solutions. The same can be said for the comparison carried out with respect to the IVS official combined polar motion solution. These results show that our VLBI solution is not really at the level of international solutions regarding polar motion. On the other hand, the results obtained for  $UT1$  ( $111$  and  $137 \mu\text{s}$  for  $UT1$  and for  $UT1$  only computed with the intensive session data) are very close (even better in the second case) to the mean values obtained for the international solutions. However, we must notice that some solutions exhibit weighted standard deviation values under the  $100 \text{ } 0.1 \mu\text{s}$  level (AUS, IAA, and SPBU solutions in Table 11). The values obtained with respect to the IVS official combined solution ( $132$  and  $155 \text{ } 0.1 \mu\text{s}$ , respectively) are also satisfactory. Finally, we can notice that all the VLBI analysis centers estimate celestial pole  $d\psi$  and  $d\varepsilon$

offsets. Owing to an inability of GINS software, we do not estimate these offsets. It can be a reason to explain the relatively middle quality of our solution.

#### 4.1.3. SLR Solutions

[44] As shown in Table 11, the results for SLR are relatively heterogeneous. Indeed, the CSR and DUT solutions are really incoherent with the three other ones and especially with the ILRS official combined solution. The mean biases with respect to EOPC04 series are  $-366 \mu\text{as}$  for  $x_p$  and  $-178 \mu\text{as}$  for  $y_p$  but, once again, the significant heterogeneities make the interpretation of results difficult. The ILRS official combined solution also exhibits significant biases. It is also the case for our solution. Indeed, the bias for  $y_p$  ( $210 \mu\text{as}$ ) is very close to the value obtained for the ILRS official combined solution ( $203 \mu\text{as}$ ). The weighted standard deviation values with respect to EOPC04 series are, on the average,  $264 \mu\text{as}$  for  $x_p$  and  $272 \mu\text{as}$  for  $y_p$ . SLR appears to be significantly less sensitive to pole coordinates than GPS and VLBI are. Regarding our solution, the weighted standard deviation values of the differences with respect to EOPC04 series ( $245 \mu\text{as}$  for  $x_p$  and  $208 \mu\text{as}$  for  $y_p$ ) are better than the mean values obtained for the international solutions. Furthermore, taking into account the heterogeneity of SLR solutions in Table 11, we can remark that the values obtained for our solution are at the mean level of international solutions, although if the two centers (IAA and MCC) for which the values obtained are the best ones also estimate  $LOD$  as a complementary parameter. Moreover, the values obtained by comparison with the ILRS official combined solution are also satisfactory.

**Table 12.** Statistics (Weighted Mean/Weighted Standard Deviation Values) of the Differences Between Our Combined Solutions With a Daily Sampling and EOPC04 (“comb.-C04”) and the IGS (“comb.-IGS”) Official Combined Time Series<sup>a</sup>

Comb.- C04	W. Mean	W. Std.	Comb.- IGS	W. Mean	W. Std.
$x_p$	-31	90	$x_p$	-9	100
$y_p$	159	92	$y_p$	-68	86
$UT1$	-11	121	$UT1$	.	.

<sup>a</sup>Units are  $\mu\text{as}$  for  $x_p$  and  $y_p$  and  $0.1 \mu\text{s}$  for  $UT1$ .

#### 4.1.4. DORIS Solutions

[45] Only two DORIS solutions contribute operationally to the computation of EOPC04 time series: our solution and the JPL solution (see Table 11). The comparison of these two solutions with respect to EOPC04 time series show weighted standard deviation values at the same level for  $y_p$ , but the JPL analysis center estimates  $LOD$  as an additional parameter.

#### 4.2. Combination Results

[46] Figure 7 shows the daily EOP offset time series computed with SLR and the combination of the four techniques, respectively. These offsets are computed with respect to the a priori models given in relations (1). This figure is sufficient to prove the efficiency of our combination. Indeed, we can clearly see a drift in the  $UT1$  offset time series computed by SLR. This drift is mainly due to the dynamic method used to carry out the SLR computations. It is impossible, in orbital signals sensed by artificial satellites, to discriminate longitudes of ascending nodes from  $UT1$ . Consequently, estimating orbital parameters together with station positions and EOPs induces strong correlations between these parameters (and, through them, the longitude of the ascending node) and  $UT1$ . As a consequence, values computed for  $UT1$  do not really make physical sense. On the other hand, Figure 7 shows that mixing partial derivatives of all techniques cancels existing correlations for satellite techniques with the help of the absolute information brought in by VLBI.

##### 4.2.1. General Analysis

[47] Table 12 shows the weighted mean and weighted standard deviation values of the differences between our combined solutions with a daily sampling and EOPC04 and the IGS official combined time series. The results in Table 12 are very satisfactory, compared to the results obtained for the individual techniques. Indeed, the weighted standard deviation values for polar motion are better than the best values obtained for any of our individual solutions in Table 11. The weighted standard deviation value for  $UT1$  is close to the value obtained with VLBI only, even if it is a little bit larger ( $121 \text{ } 0.1 \mu\text{s}$  against  $111$  for VLBI). Furthermore, the values in Table 12 show a significant bias ( $159 \mu\text{as}$  to  $5 \text{ mm}$ ) for  $y_p$ , equal to the previous value found with GPS (see Table 11). This bias demonstrates that the reference underlying our EOP estimations is mainly due to GPS. Indeed, as previously seen, this technique is highly weighted in the combination and highly sensitive to polar motion. Figure 8 shows the daily EOP offset time series for the individual techniques and the combination of techniques. We can notice the similarity between the GPS and combined solutions for

polar motion. Indeed, the weighted standard deviation values of the differences between these two time series are  $44 \mu\text{as}$  for  $x_p$  and  $41 \mu\text{as}$  for  $y_p$  (nearly  $1 \text{ mm}$ ). GPS clearly dominates the three others techniques in the combination regarding pole coordinates. Regarding  $UT1$ , although they do not have the same sampling, the VLBI and combined solutions are comparable. Furthermore, the VLBI solution does not have a regular sampling. The combination has it, with a comparable weighted standard deviation value. Finally, we can notice in Table 12 that the standard deviation value of the difference between our combined series and the IGS official combined solution is lower for  $y_p$  than the value obtained with respect to EOPC04 series. This result is encouraging. Indeed, the IGS official combined polar motion series better correlate with independent geophysical series than EOPC04 series do [Kouba, 2005].

##### 4.2.2. Particular Analysis of the 6-Hour Solutions

[48] We have carried out spectral analyses over our 6-hour EOP offset combined time series. These analyses are based on the software Frequency Analysis Mapping on Unusual Sampling (FAMOUS), developed by F. Mignard (OCA) in the framework of GAIA project [Mignard, 2004]. This software detects periodic signals in time series and computes frequencies and amplitudes of these signals. Such preliminary spectral analyses show a significant diurnal signal (the period is close to  $1.0027$  days,  $1$  sidereal day) for pole coordinates  $x_p$  and  $y_p$ . This diurnal signal found in pole coordinates is in fact a retrograde signal as shown in Figure 9. This signal has already been detected [Watkins and Eanes, 1994; Hefty et al., 2000].

[49] This artificial signal is due to the correlation between orbital parameters and diurnal retrograde signals in polar motion. It can appear when nutation offsets are not computed [Hefty et al., 2000]. Also, owing to an inability of GINS software, nutation offsets are not parameters of our experiment. This artefact can be eliminated by applying appropriate constraints. A physical retrograde signal of frequency  $\omega$  and phase  $\varphi$  in polar motion can be modelled as follows:

$$\begin{cases} x_p = \rho \cos(\omega t + \varphi) \\ y_p = \rho \sin(\omega t + \varphi). \end{cases}$$

or, with  $\rho_c = \rho \cos \varphi$  and  $\rho_s = \rho \sin \varphi$ ,

$$\begin{pmatrix} x_p \\ y_p \end{pmatrix} = \begin{bmatrix} \cos \omega t & -\sin \omega t \\ \sin \omega t & \cos \omega t \end{bmatrix} \cdot \begin{pmatrix} \rho_c \\ \rho_s \end{pmatrix} \quad (5)$$

[50] Thus we can cancel any retrograde signal with the constraints

$$(A^T A)^{-1} \begin{pmatrix} \rho_c \\ \rho_s \end{pmatrix} = 0 \begin{pmatrix} \sigma^2 & 0 \\ 0 & \sigma^2 \end{pmatrix} \quad (6)$$

the matrix  $A$  resulting from the gathering of the daily systems (5) over 1 week. As shown in the power spectra in Figure 9, these constraints successfully eliminate the artefact in the combined solutions. The removal of this artificial diurnal retrograde signal strongly decreases the weighted standard deviation values of the differences between our 6-hour solutions and EOPC04 and the IGS official combined time series as shown in Table 13.

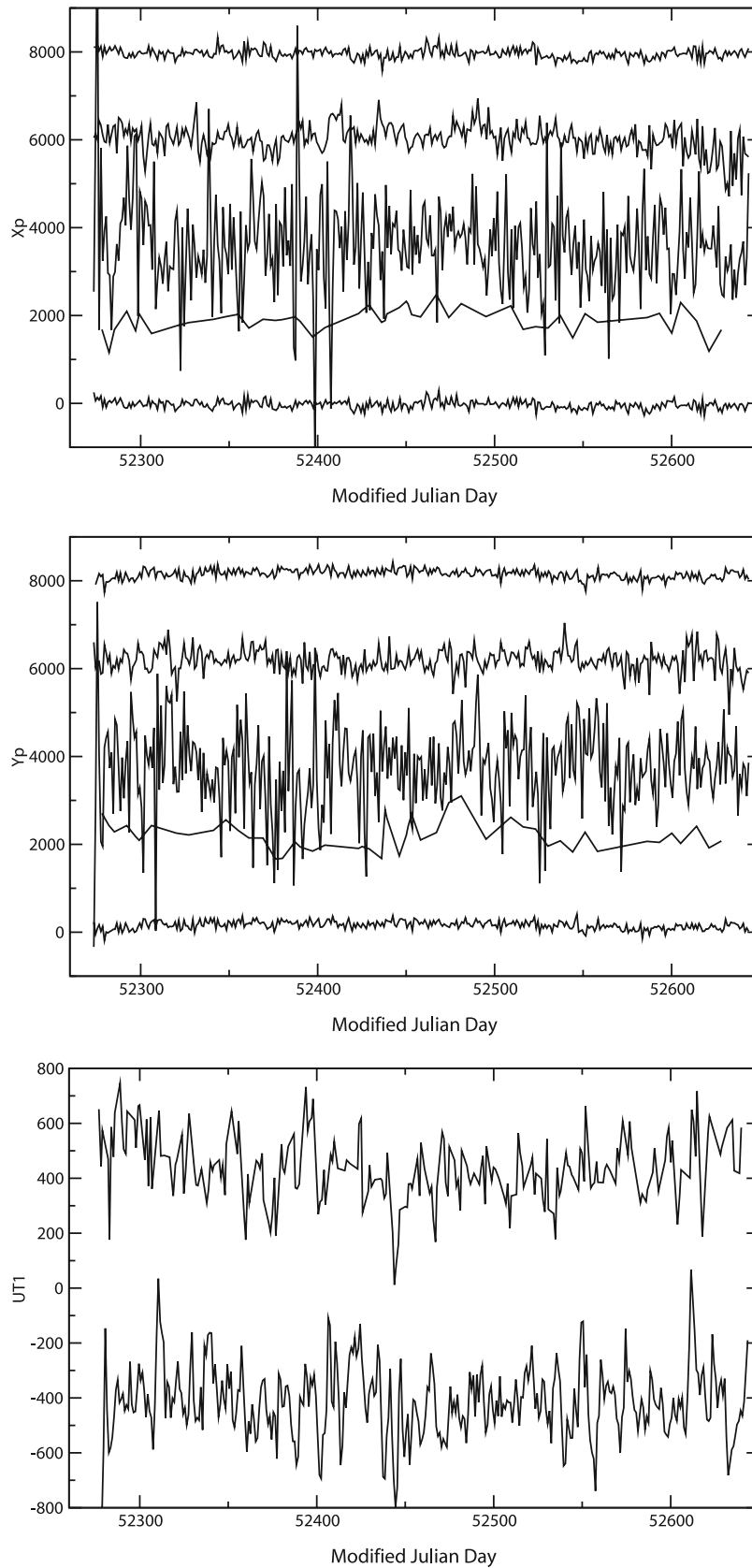


**Figure 8.** Daily EOP offset time series for individual techniques and the combination. From top to bottom,  $x_p$ ,  $y_p$ , and  $UT1$ . For polar motion, from top to bottom, GPS, SLR, DORIS, VLBI, and the combination. For  $UT1$ , from top to bottom, VLBI and the combination. Units are  $\mu\text{s}$  for polar motion and  $0.1 \mu\text{s}$  for  $UT1$ .

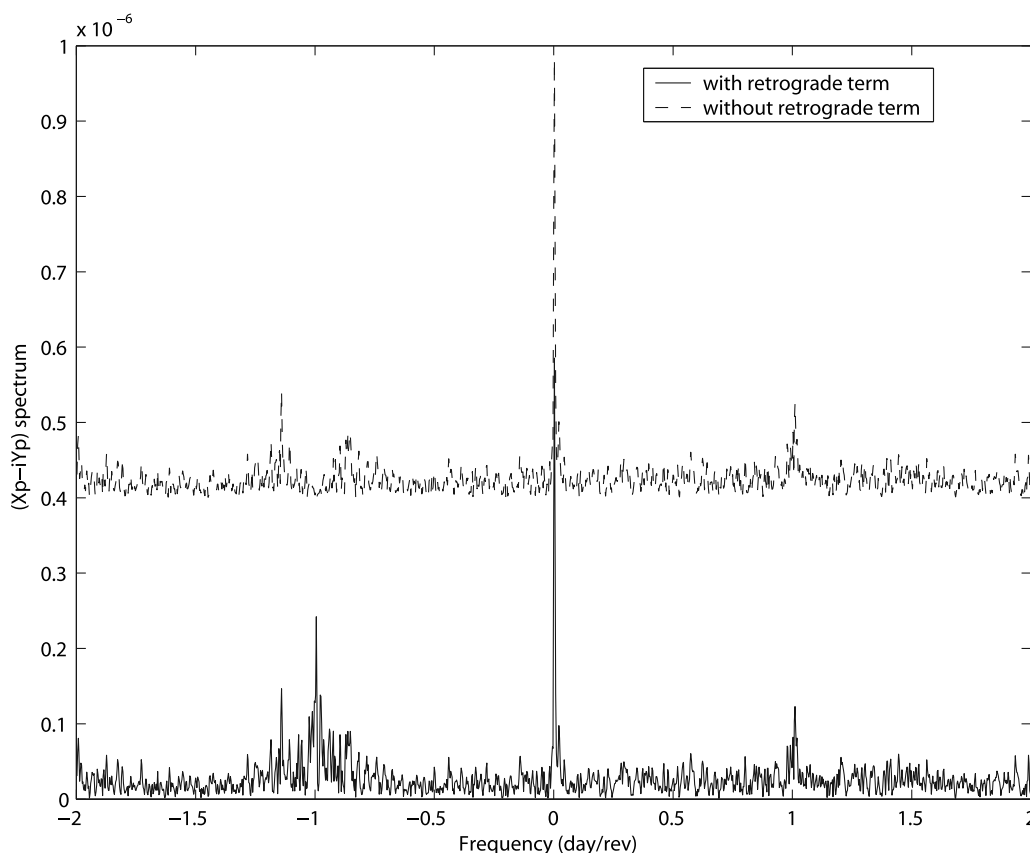


**Figure 9.** Prograde and retrograde power spectra of the differences between the combined 6-hour polar motion time series and EOPC04 series. The negative (positive) frequencies correspond to the retrograde (prograde) spectrum. The continuous (dashed) curve corresponds to the 6-hour solution before (after) the removal of the artificial retrograde signal.

[51] We can notice in Table 13 that our 6-hour solutions produced after the removal of the diurnal retrograde artefact have very satisfactory weighted standard deviation values with respect to EOPC04 and the IGS official combined time series (the values are at the same level). Furthermore, the value obtained for *UT1* (152  $\mu$ s) shows the quality of our combined *UT1* solution (with respect to our VLBI solution) computed with a 6-hour sampling (to be compared with the discontinuous sampling provided by VLBI only).

## 5. Toward Combined TRFs

### 5.1. Individual TRFs

[52] Table 15 lists all the reference system effects computed for the DORIS, GPS, SLR, and VLBI techniques. These effects are related to (1) the weekly solutions of station positions alone (EOPs are held fixed) computed with weak constraints of 1 m, (2) the weekly solutions of EOPs (with a daily sampling) and station positions derived with weak constraints of 1 m, (3) the solutions of EOPs (with a daily sampling) and station positions derived with minimum constraints applied on station positions. Regarding these minimum constraints, Table 15 also indicates, for each technique, the parameters for which these constraints are applied. These parameters correspond to the parameters which exhibit significant reference system effects (the bold values in Table 15).

[53] In order to make the weekly references underlying the EOP estimates homogeneous over the whole year 2002, we apply minimum constraints with respect to ITRF2000. Furthermore, we use well distributed subnetworks per technique to apply these constraints each week. Table 14 lists these minimum networks for each technique. The method used to find these optimal networks is the following:

[54] 1. First, we computed EOPs and station positions with very weak constraints of 10 km. Then, we computed the seven-parameter transformations between the weekly TRFs

**Table 13.** Statistics (Weighted Mean/Weighted Standard Deviation Values) of the Differences Between Our 6-Hour Combined EOP Time Series Before and After the Removal of the Artificial Retrograde Signal and EOPC04 and the IGS Official Combined Time Series<sup>a</sup>

Solution	$x_p$	$y_p$	<i>UT1</i>
Comb.- EOPC04	-28/234	165/215	-20/152
Comb.- EOPC04 const. <sup>b</sup>	-28/197	166/193	-20/152
Comb.- IGS	-5/238	-64/218	.
Comb.- IGS const.	-5/202	-64/196	.

<sup>a</sup>Units are  $\mu$ as for  $x_p$  and  $y_p$  and 0.1  $\mu$ s for *UT1*.

<sup>b</sup>Here “const.” corresponds to the 6-hour combined solutions after the removal of the artificial diurnal retrograde signal produced with the constraints (6).

**Table 14.** Subnetworks Used to Apply Minimum Constraints With Respect to ITRF2000 for the Four Techniques<sup>a</sup>

DOMES	Code	Name	Location	T <sup>b</sup>	Longitude	Latitude
10003S003	TLHA	Toulouse	France	D	1.485	43.550
10317S004	SPIB	Ny Alesund	Norway	D	11.932	78.9234
12329S001	SAKA	Sakhalins	Russia	D	142.717	47.030
12334S006	KIUB	Kitab	Uzbekistan	D	66.885	39.135
12349S001	KRAB	Krasnoyarsk	Russia	D	92.794	55.993
23501S001	COLA	Colombo	Sri Lanka	D	79.874	6.892
30302S006	HBKB	Hartebeesthoek	South Africa	D	27.708	-24.113
30604S002	TRIB	Tristan Da Cunha	United Kingdom (South Atlantic ocean)	D	348.313	-36.935
39801S005	MAHB	Mahe Island	Seychelles	D	55.531	-3.321
40127S008	YELB	Yellowknife	Canada	D	246.480	62.481
40408S005	FAIB	Fairbanks	United States (Alaska)	D	213.518	64.973
40424S008	KOKA	Kauai	United States (Hawai)	D	201.665	22.123
41703S009	EASB	Easter Island	Chile	D	251.384	-26.852
50207S001	CHAB	Chatham Island	New Zealand	D	184.566	-42.044
66006S003	SYPB	Syowa	Antarctica (Japanese base)	D	39.579	-68.995
91201S004	KESB	Kerguelen	France (French Southern and Antartic lands)	D	70.256	-48.648
91401S003	AMTB	Amsterdam	France (French Southern and Antartic lands)	D	77.571	-36.201
92902S001	FUTB	Futuna	France (Wallis and Futuna)	D	182.121	-13.692
12352M001	SELE	Almaty	Kazakstan	P	77.017	43.179
12360M001	TIXI	Tixi	Russian Federation	P	128.866	71.635
13504M003	KOSG	Kootwijk (near Apeldoorn)	Netherlands	P	5.810	52.178
21613M001	LHAS	Lhasa	China	P	91.104	29.657
30302M004	HRAO	Krugersdorp	South Africa	P	27.687	-24.110
30314M002	SUTH	Sutherland	South Africa	P	20.811	-31.620
40400M007	JPLM	Pasadena	United States	P	242.173	34.205
40442M012	MDO1	Fort Davis	United States	P	256.015	30.681
40477M001	MKEA	Mauna Kea	United States	P	205.456	19.801
41703M003	EISL	Easter Island	Chile	P	251.383	-26.852
43201M001	CRO1	Christiansted	United States (Virgin Islands)	P	296.584	17.757
50103M108	TIDB	Tidbinilla	Australia	P	148.980	-34.601
50127M001	COCO	Cocos (Keeling) Island	Australia	P	96.834	-11.812
50207M001	CHAT	Waitangi	New Zealand	P	184.566	-42.044
11001S002	7839	Graz	Austria	L	15.493	47.067
13212S001	7840	Herstmonceux	United Kingdom	L	0.336	50.867
30302M003	7501	Hartebeesthoek	South Africa	L	27.686	-24.110
40451M105	7105	Greenbelt	United States	L	284.828	39.021
40497M001	7110	Monument Peak	United States	L	244.423	32.892
50107M001	7090	Yarragadee	Australia	L	115.347	-28.954
50119S001	7849	Mount Stromlo	Australia	L	149.010	-34.684
12734S005	7243	Matera	Italy	R	16.704	40.650
14201S004	7224	Wetzell	Germany	R	12.877	49.145
21605S009	7227	Shanghai	China	R	121.200	31.099
40104S001	7282	Algonquin Park	Canada	R	282.073	45.956
40424S007	7298	Kokee Park	United States	R	201.665	22.127
41602S001	7297	Fortaleza	Brazil	R	322.426	-2.122
50116S002	7242	Hobart	Australia	R	147.441	-41.196

<sup>a</sup>For each instrument, its DOMES number, its CDDIS code, its name, its geographical location (country), the technique involved, and its geographical coordinates are listed. Unit is degree for longitude and latitude.

<sup>b</sup>“D” corresponds to DORIS, “P” corresponds to GPS, “L” corresponds to SLR, and “R” corresponds to VLBI.

and ITRF2000. To do this, we eliminated the stations for which the estimation residuals were larger than 5 cm (3 cm) for DORIS, SLR, and VLBI (GPS). The stations which were eliminated in less than 26 weeks were kept.

[55] 2. Second, among these networks, we only kept the stations for which the positions were at least computed for 37 weeks.

[56] 3. Finally, among these “good” stations, we searched for the subnetworks which minimized the reference system effects over the whole year 2002.

[57] On the basis of these minimum networks, minimum constraints are applied at a 0.1 mm level. Indeed, numerical tests showed that it was an optimal value to really cancel the reference system effects. Regarding the weekly solutions of station positions alone, the results in Table 15 show predictable reference system effects. Indeed, all the satellite

techniques exhibit a strong effect for the third rotation due to the dynamic approaches used to derive the solutions. This effect is not present for VLBI. For this technique, strong effects affect the three translations, highlighting the insensitivity of VLBI to geocenter. On the other hand, we can notice significant effects on the third translation for the DORIS and GPS techniques. This effect is certainly due to the geometry of DORIS measurements on the satellites used. Indeed, DORIS network has the best distribution. A bad definition of any degree of freedom of the TRF can only be linked to the satellite constellation involved. For GPS, we know (see section 2.3) that the network effectively used can present a small number of receivers (nearly 50) for some weeks. This can give rise to singularities in computations. Finally, SLR shows, through the effects on the three translations, its ability to derive geocenter motion. Never-

**Table 15.** Mean Reference System Effects Over the Year 2002 for the Weekly DORIS, GPS, SLR, and VLBI Solutions, cm

Solution	Effect	$T_x$	$T_y$	$T_z$	$D$	$R_x$	$R_y$	$R_z$
DORIS stations (weak constraints <sup>a</sup> )	stations	0.13	0.13	<b>0.54</b> <sup>b</sup>	0.13	0.43	0.41	<b>18.52</b>
DORIS EOPs + stations (weak constraints)	EOPs	.	.	.	.	<b>16.51</b>	<b>16.77</b>	.
DORIS EOPs + stations (weak constraints)	stations	0.13	0.13	<b>0.54</b>	0.14	<b>16.50</b>	<b>16.77</b>	<b>18.52</b>
Constrained parameters <sup>c</sup>		.	•	.	•	•	•	.
DORIS EOPs + stations (minimum constraints <sup>d</sup> )	EOPs	.	.	.	.	0.51	0.47	.
DORIS EOPs + stations (minimum constraints)	stations	0.13	0.13	0.02	0.13	0.02	0.02	0.05
GPS stations (weak constraints)	stations	0.07	0.07	<b>0.39</b>	0.02	0.02	0.02	<b>3.35</b>
GPS EOPs + stations (weak constraints)	EOPs	.	.	.	.	<b>3.64</b>	<b>3.75</b>	.
GPS EOPs + stations (weak constraints)	stations	0.08	0.07	<b>0.39</b>	0.02	<b>3.64</b>	<b>3.75</b>	<b>3.42</b>
Constrained parameters		.	•	.	•	•	•	.
GPS EOPs + stations (minimum constraints)	EOPs	.	.	.	.	0.03	0.04	.
GPS EOPs + stations (minimum constraints)	stations	0.07	0.07	0.01	0.02	0.01	0.02	0.01
SLR stations (weak constraints)	stations	0.05	0.05	0.13	0.04	0.07	0.07	<b>29.34</b>
SLR EOPs + stations (weak constraints)	EOPs	.	.	.	.	<b>2.93</b>	<b>1.59</b>	.
SLR EOPs + stations (weak constraints)	stations	0.05	0.05	0.12	0.03	<b>2.67</b>	<b>1.43</b>	<b>26.20</b>
Constrained parameters		.	.	.	•	•	•	.
SLR EOPs + stations (minimum constraints)	EOPs	.	.	.	.	0.10	0.13	.
SLR EOPs + stations (minimum constraints)	stations	0.05	0.05	0.12	0.04	0.02	0.04	0.02
VLBI stations (weak constraints)	stations	<b>38.18</b>	<b>38.18</b>	<b>38.18</b>	0.25	0.19	0.22	0.09
VLBI EOPs + stations (weak constraints)	EOPs	.	.	.	.	<b>0.63</b>	<b>0.57</b>	<b>29.14</b>
VLBI EOPs + stations (weak constraints)	stations	<b>38.28</b>	<b>38.15</b>	<b>37.80</b>	0.25	<b>0.69</b>	0.57	29.13
Constrained parameters		•	•	•	.	•	•	•
VLBI EOPs + stations (minimum constraints)	EOPs	.	.	.	.	0.46	0.39	0.18
VLBI EOPs + stations (minimum constraints)	stations	0.04	0.05	0.11	0.25	0.01	0.01	0.01

<sup>a</sup>Constraints to zero at the level of 1 m for station positions and EOPs.

<sup>b</sup>Doubtful values are bold.

<sup>c</sup>Black disks indicate the parameters for which minimum constraints are applied.

<sup>d</sup>Minimum constraints are applied with respect to ITRF2000 at the level of 0.1 mm.

theless, we can notice the larger effect on  $T_z$  probably due to the bad distribution of SLR stations (Figure 3). Solutions for EOPs and station positions derived with weak constraints of 1 m show new effects regarding the orientation of TRFs; the reference system effects for EOPs are computed with relations (4). This effect is predictable as, estimating EOPs together with station positions, the orientation of the underlying TRF is not defined at all. Finally, regarding the solutions computed with minimum constraints, we can notice that the reference system effects derived from EOP and station position variance matrices are no more coherent. Indeed, the values are always a little bit larger for EOPs but the effects are not so strong (typically a few millimeters): consult section 5.2 for a discussion of this fact. These reference system effects are below the millimeter level for station positions. Indeed, the values are close to 0.1 mm (the maximum value is 0.5 mm), the level at which minimum constraints are applied. Table 16 shows the mean values and the mean standard deviation values of the seven transformation parameters between the individual solutions computed with minimum constraints and ITRF2000.

[58] Values obtained for DORIS are rather large for the two first translations but we can especially notice the large bias for the scale factor, already highlighted by other groups [Willis *et al.*, 2007]. The standard deviation values are at the level of a few millimeters, probably due to the good geographic distribution of the DORIS beacons. Regarding GPS, we can notice some large standard deviation values. These values close to 1 cm are certainly due to deficiencies in the reduced network we use. The values are satisfactory for SLR which exhibits the smallest standard deviation values for the two first translations in comparison with the other satellite techniques. On the other hand, the very large

value (more than 1 cm) obtained for the third translation can certainly be linked to the bad distribution of the SLR network, and, as a consequence, to the relatively bad distribution of the subnetwork used to apply minimum constraints. The rotation standard deviation values at the centimeter level show the difficulty for this technique to derive the orientation of its underlying TRFs. Moreover, we can notice the small mean value obtained for the scale factor (1.5 mm), proof of a robust estimation of range biases. Finally, the values are relatively small for VLBI for which the results in Table 16 show the smallest standard deviation values for the three rotations. This shows the great ability of this technique to derive the orientation of TRFs in space. Regarding the three rotations, we can notice the small values obtained (less than 0.1 mm for VLBI and up to 4 mm for SLR). This shows the effectiveness of minimum

**Table 16.** Mean Values and Mean Standard Deviation Values of the Seven Estimated Parameters of Transformation Between Our Individual Solutions Computed With Minimum Constraints and ITRF2000, cm

Parameter	$T_x$	$T_y$	$T_z$	$D$	$R_x$	$R_y$	$R_z$
DORIS values	-0.84	-2.50	-0.32	4.66	-0.16	0.05	-0.18
DORIS $\sigma^a$	0.48	0.47	0.06	0.49	0.08	0.08	0.20
GPS values	-0.25	-0.01	-0.18	1.41	0.01	0.06	-0.01
GPS $\sigma$	0.95	0.94	0.07	0.29	0.18	0.22	0.10
SLR values	-0.17	0.39	1.59	0.15	0.01	0.38	-0.21
SLR $\sigma$	0.45	0.44	1.18	0.33	0.18	0.36	0.21
VLBI values	0.00	-0.10	0.12	-0.38	0.00	0.00	0.00
VLBI $\sigma$	0.15	0.22	0.44	0.95	0.04	0.04	0.04

<sup>a</sup>Here “ $\sigma$ ” corresponds to the mean standard deviation value of the estimations.

**Table 17.** Reference System Effects Computed Through the Variance Matrices of EOPs and Station Positions for the First Weekly SLR EOP and Station Position Solution Computed With Weak Constraints of 1 m<sup>a</sup>

Parameter	Standard Deviation	Internal Noise
$x_p$ (mean)	1.44	0.03
$y_p$ (mean)	0.40	0.04
$R_X$ EOPs <sup>b</sup>	0.39	.
$R_Y$ EOPs	1.42	.
$R_X$ stations <sup>c</sup>	0.38	.
$R_Y$ stations	1.37	.

<sup>a</sup>Unit is mas. For EOPs, the mean standard deviation values and the mean internal noises are translated into standard deviation values. The reference system effects for the two rotations are translated into standard deviation values.

<sup>b</sup>The reference system effect is derived from the variance matrix of EOPs.

<sup>c</sup>The reference system effect is derived from the variance matrix of station positions.

constraints. Nevertheless, the biases obtained for DORIS and SLR (at the level of a few millimeters) also show the limits of such constraints.

## 5.2. Minimum Constraints and EOPs

[59] As shown in Table 15, reference system effect affects not only station positions materializing the considered TRF but also EOPs computed with respect to the three axes of this TRF. As an example, Table 17 shows the reference system effect on the two rotations  $R_X$  and  $R_Y$  computed through the variance matrices of EOPs and station positions for the first weekly SLR EOP and station position solution computed with weak constraints of 1 m.

[60] Table 17 shows the great agreement between the reference system effects derived from the variance matrices of EOPs and station positions, respectively. This can also be seen in Table 15. So, the reference system effect affects EOPs at the same level as it does station positions. Minimum constraints fully eliminate the reference system effect on station positions. These constraints should also eliminate the reference system effect on EOPs.

[61] Taking again the weekly SLR normal system of Table 17, we add minimum constraints (see section 5.1 for details) and invert the normal system obtained to derive EOPs and station positions. If the reference system effect clearly disappears for station positions, it is not the case for EOPs. Indeed, the mean standard deviation values are 0.88 mas for  $x_p$  and 0.30 mas for  $y_p$ . Minimum constraints do not fully eliminate the reference system effect for EOPs.

[62] Further investigations on this normal system show that a few stations bring a small number of measurements during this particular week. By eliminating these stations during SLR orbit computations (section 2.4), minimum constraints are now sufficient to significantly reduce the reference system on EOPs. The network used to derive EOPs has a great importance and much attention must be paid to it. Moreover, the geometric distribution of measurements also plays an important role in this problem.

[63] As noticed in section 5.1, Table 15 lists the mean reference system effects over the year 2002 for our individual daily EOP solutions computed together with station positions under minimum constraints in agreement with Figure 5.

**Table 18.** Mean Reference System Effects Computed Through the Variance Matrices of Station Positions of the Weekly Combined EOP and Station Position Solutions Estimated With Weak Constraints at 1 m<sup>a</sup>

Parameter	Effect
$T_X$	0.03
$T_Y$	0.03
$T_Z$	0.10
$D$	0.02
$R_X$	<b>7.45</b>
$R_Y$	<b>7.03</b>
$R_Z$	<b>8.13</b>

<sup>a</sup>The effects are translated into standard deviation values of the seven parameters. Unit is cm.

[64] Minimum constraints being applied, the TRF underlying the estimation of EOPs should be correctly defined. This is not always the case as shown in Table 15. The values in this table can thus be interpreted as sensitivities of techniques to EOPs. Indeed, a significant reference system effect in the variance matrices of EOPs, although the TRF is well defined, proves the difficulty, through our analysis, for the considered technique, to define the reference underlying the EOP estimations it provides.

[65] Furthermore, the effects in Table 15 can be understood as criteria of the quality of the station network used. Indeed, the values are very small for GPS, the technique which is very sensitive to polar motion and for which we have a well distributed network, even if it is a reduced one. The results obtained for DORIS are very interesting. Although this technique has the best network, it produces the strongest reference system effects. These effects are in fact due to the weak sensitivity of DORIS to pole coordinates. The results for SLR and VLBI also make sense. SLR is known to be less sensitive to Earth rotation than VLBI, but its ground network is better distributed than the VLBI one (see maps in Figure 3 and Figure 4). Finally, we can notice the relatively small effect (2 mm) on the third rotation  $R_Z$  for VLBI. This value shows the great sensitivity of this technique to  $UT1$ , a sensitivity which is stronger than those to polar motion. Sensitivities of techniques with respect to EOPs given through these reference system effects can also be directly linked to the celestial objects observed by these techniques. Indeed, the distribution of the orbital planes of the satellites is of great importance for DORIS, GPS, and SLR, as is the geometric distribution of the extragalactic quasars for VLBI.

## 5.3. Combined TRFs

[66] By mixing the weekly individual normal systems (see Figure 5), we obtain the weekly combined normal systems related to both EOPs and station positions.

**Table 19.** Mean Reference System Effects Computed Per Technique Inside the Combination Through the Variance Matrices of Station Positions of the Weekly Combined EOP and Station Position Solutions Estimated With Weak Constraints of 1 m<sup>a</sup>

Technique	$T_X$	$T_Y$	$T_Z$	$D$	$R_X$	$R_Y$	$R_Z$
DORIS	0.09	0.09	<b>0.38</b>	0.09	<b>8.03</b>	<b>7.41</b>	<b>17.40</b>
GPS	0.07	0.07	<b>0.39</b>	0.02	<b>8.01</b>	<b>7.40</b>	<b>15.59</b>
SLR	0.04	0.04	0.11	0.03	<b>8.01</b>	<b>7.39</b>	<b>23.04</b>
VLBI	<b>41.31</b>	<b>41.29</b>	<b>40.98</b>	0.19	<b>7.72</b>	<b>8.21</b>	<b>15.41</b>

<sup>a</sup>The effects are translated into standard deviation values of the seven parameters. Unit is cm.

**Table 20.** Mean Values of the Seven Transformation Parameters Estimated Per Technique Between the Combined Weekly TRF Solutions Computed With Minimum Constraints and ITRF2000, cm

Parameter	$T_X$	$T_Y$	$T_Z$	$D$	$R_X$	$R_Y$	$R_Z$
DORIS	-0.69	-2.00	-0.26	3.69	-0.13	0.04	-0.15
GPS	-0.22	0.03	-0.16	1.17	0.01	0.05	-0.01
SLR	-0.14	0.27	0.92	0.14	0.00	0.23	-0.14
VLBI	0.00	-0.10	0.13	-0.40	0.00	0.00	0.01

[67] These weekly combined normal systems are not invertible. Indeed, Table 18 (which lists the mean reference system effects for the weekly combined EOP and station position solutions computed with weak constraints of 1 m) shows that the three rotations exhibit a significant effect.

[68] To eliminate the reference system effect of Table 18, we add minimum constraints for the three rotations with respect to ITRF2000. Doing so gives realistic standard deviation values for the positions of GPS sites, but the standard deviation values for the station positions related to the three other techniques are still very large.

[69] Table 19 shows the mean reference system effects per technique inside the weekly combined EOP and station position solutions estimated with weak constraints. These effects show that the individual techniques exhibit the same reference system effects in the combination as they do alone (Table 15). In order to solve this problem, we decided to not combine the weekly individual normal systems but the weekly normal systems regularized by minimum constraints per technique (see Figure 5). Minimum constraints are applied with respect to ITRF2000 and are related to the parameters for which the effects are significant (the bold values in Table 19). We keep the subnetworks used for the individual computations (Table 14) to apply these minimum constraints. This provides weekly combined TRFs for which the standard deviation values on station positions and EOPs are satisfactory.

[70] However, as shown in Table 20, the individual techniques still realize their own TRFs inside the combination. The combined TRFs are not homogeneous although EOPs, as common parameters for all techniques, probably homogenize the individual rotation parameters. Indeed, the reference system effects for the two rotations  $R_X$  and  $R_Y$  in Table 19 are homogeneous in comparison to those shown in Table 15. This heterogeneity completely prevented us from using local ties and, as a consequence, colocated station positions to link techniques.

#### 5.4. Prospects

[71] A solution to the previous problem can consist in constraining the individual weekly TRFs to be realized in ITRF2000. However, doing so clearly transgresses physics of measurements and gives rise to inaccuracies in the computations. Another solution is based on alternative computation models. Indeed, parameters worthy of interest will be no more EOPs and station positions, but EOPs and station positions in a combined homogeneous TRF together with the seven individual transformation parameters between the TRFs underlying measurements of techniques

and this combined TRF. Such an approach is used for the ITRF computation [Altamimi *et al.*, 2002a] albeit at the level of individual solutions.

[72] In our case, such a model will be directly derived at the observational level. Furthermore, this approach should reduce the heterogeneities between the references for EOPs and station positions highlighted in sections 5.1 and 5.2. Indeed, the main problem regarding EOPs and the rotation parameters derived from station positions consists in finding the station network for which the measurements are really used to compute EOPs. However, for any given station, all the measurements do not necessarily have the same quality. Estimating transformation parameters at the level of measurements should make possible, through an optimal data weighting, to derive exactly EOPs linked to the combined TRF.

## 6. Conclusions

[73] This experiment of space-geodetic technique combination at the normal system level is the first computation of such importance carried out by the French GRGS in the field of terrestrial reference systems. Moreover, it is clearly a first step towards a direct combination at the measurement level. Although we were unable to consider nutation offsets as parameters, our combination shows clearly its strength for the EOP determination. Indeed, the standard deviation values of the combined solutions are better or at the level of those obtained for our individual solutions. Also, the comparisons of these individual solutions with the international analysis center solutions show that our DORIS and SLR solutions are at the level of international solutions. On the other hand, they also show that our GPS and VLBI solutions are at the level of international solutions for which standard deviation values of differences with respect to EOPC04 or official combined time series are the largest ones. However, in this paper the quality of individual computations was not crucial as the concept of all-combined solutions was clearly the important point. Nevertheless, we plan, in the very near future, to upgrade GINS software to carry out better GPS and VLBI data processings. On the other hand, it must be noticed that GINS is probably the only software in the worldwide geodetic community which permits to carry out computations with all the geodetic techniques used to derive official IERS EOPs and TRFs. Moreover, in the near future, comparisons with international analysis center solutions should be carried out not only on the basis of EOPs but also of station positions.

[74] When our individual GPS and VLBI computations will reproduce the state-of-the-art data processings, we should be able to carry out physical interpretations of EOP offset time series, over a longer period of time (typically over several years). In this framework, amplitudes of periodic variations due to oceanic and zonal tides could be directly determined through measurements. Such approaches have already been used [Watkins and Eanes, 1994; Hefy *et al.*, 2000]. We should also compare our combined EOP series with geophysical excitations such as Oceanic and Atmospheric Angular Momenta as it is done by Kouba [2005]. In this context of EOP computation, nutation offsets must be parameters worthy of interest in the future developments linked to this experiment. Indeed, as is

the case for *UT1* in the present paper, partial derivatives of satellite techniques (even if they are low) could be mixed with those of VLBI. All these computations linked to EOPs will be the core of a next investigation.

[75] Concerning the realization of combined TRFs, improvements should be made in the model used in order to take into account (and to eliminate) the remaining biases between individual techniques in the combined normal systems. Such a model should link techniques in a real combined homogeneous TRF. So, we could use (and validate) local ties in IERS collocation geodetic sites and weight techniques not only through EOPs but also through station positions. Furthermore, it seems unreasonable to use local ties on a weekly basis. Indeed, using local ties in the context of weekly combinations is a completely different approach than the one consisting in applying these local ties between mean station positions computed over nearly 15 years, due to physical signals which may be revealed by the weekly station position time series. Thus we have to find an improved combination model to ensure, on the one hand, that, each week, all technique station positions are computed in the same global reference frame and, on the other hand, that local ties are used in an optimal way. Elaboration and testing of such models will be described in a future paper.

[76] Finally, research on such combinations at the observational level should be continued. Indeed, the quality presently reached by space-geodetic measurements and the next role of the European GALILEO positioning and navigation system should encourage us to reduce intermediate steps between measurements and reference products such as ITRF and EOPs. This in order to still improve the quality of these fundamental references. Moreover, taking into account new links such as multitechnique satellites, atmospheric delays (we plan to upgrade GINS to derive common zenithal delays based on homogeneous mapping functions for the techniques involved) in collocation sites, and geocenter motion should also improve such combinations. This is of particular importance because main geodetic reference products such as ICRF, ITRF, EOPs, and Earth gravity field should be derived from these combinations.

[77] **Acknowledgments.** This work was supported by the French Groupe de Recherche en Géodésie Spatiale (GRGS) and, more particularly, by the French Institut Géographique National (IGN -Saint-Mandé, France), the Observatoire de la Côte d'Azur (OCA -Grasse, France), the Observatoire Midi-Pyrénées (OMP -Toulouse, France), and the Paris' and Meudon's Observatory (OBSPM -Paris and Meudon, France). Fruitful discussions with members of the GRGS involved in this experiment have been found very helpful. We are particularly grateful to Z. Altamimi (IGN/LAREG), F. Barlier (OCA/GEMINI), M. Bougeard (OBSPM/SYRTE), G. Bourda (Observatory of Bordeaux), N. Capitaine (OBSPM/SYRTE), P. Charlot (Observatory of Bordeaux), P. Exertier (OCA/GEMINI), M. Feissel-Vernier (OBSPM/SYRTE and IGN/LAREG), G. Francou (OBSPM/SYRTE), D. Gambis (OBSPM/SYRTE), O. Laurain (OCA/GEMINI), J.-M. Lemoine (CNES/OMP), J.-C. Marty (CNES/OMP), P. Sillard (INSEE), and P. Yaya (CLS) for their help and relevant advice. We are especially grateful to the analysis centers of the four services IDS, IGS, ILRS, and IVS for their EOP solutions and to C. Bizouard (OBSPM/SYRTE) who masters the EOP Product Center Web site. We also acknowledge F. Mignard (OCA/CASSIOPEE) for his software FAMOUS used for spectral analyses carried out on the 6-hour combined solutions. We are very grateful to F. Barlier, P. Bonnefond, P. Exertier, and G. Métris (from OCA/GEMINI) for their readings of a preliminary version of this paper. Finally, we thank very much the two referees of the submitted version of this article, J. Ray (NOAA/NGS, USA) and R. Gross (JPL, USA): their remarks and comments helped us to not only make this paper more comprehensive and precise but also to improve our computations and results.

## References

- Altamimi, Z., P. Sillard, and C. Boucher (2002a), ITRF2000: A new release of the International Terrestrial Reference Frame for earth science applications, *J. Geophys. Res.*, *107*(B10), 2214, doi:10.1029/2001JB000561.
- Altamimi, Z., C. Boucher, and P. Sillard (2002b), New trends for the realization of the International Terrestrial Reference Frame, *Adv. Space Res.*, *30*(2), 175–184.
- Andersen, P. H. (2000), Multi-level arc combination with stochastic parameters, *J. Geod.*, *74*, 531–551.
- Aoki, S., B. Guinot, G. H. Kaplan, H. Kinoshita, D. D. McCarthy, and P. K. Seidelmann (1982), The new definition of Universal Time, *Astron. Astrophys.*, *105*, 359–361.
- Arias, E. F., P. Charlot, M. Feissel, and M. F. Lestrade (1995), The Extragalactic Reference System of the International Earth Rotation Service, *ICRS, Astron. Astrophys.*, *303*, 604–608.
- Baby, H. B., P. Gole, and J. Lavergnat (1988), A model for the tropospheric excess path length of radio waves from surface meteorological measurements, *Radio Sci.*, *23*, 1023–1038.
- Bar-Sever, Y., and D. Kuang (2003), New empirically-derived solar radiation pressure model for GPS satellites, *Geoph. Res. Abstr.*, *5*, 03248.
- Berger, C., R. Biancale, M. III, and F. Barlier (1998), Improvement of the empirical thermospheric model DTM: DTM94- a comparative review of various temporal variations and prospects in space geodesy applications, *J. Geod.*, *72*(3), 161–178.
- Coulot, D. (2005), Télémétrie laser sur satellites et combinaison de techniques géodésiques: Contributions aux systèmes de référence terrestres et applications, Ph.D. thesis, Obs. de Paris, Paris.
- Crétaux, J.-F., F. Nouel, C. Valorge, and P. Janniere (1994), Introduction of empirical parameters deduced from the Hill's equations for satellite orbit determination, *Manusc. Geod.*, *19*, 135–156.
- Exertier, P., J. Nicolas, Ph. Berio, D. Coulot, P. Bonnefond, and O. Laurain (2004), The role of Laser Ranging for calibrating Jason-1: The Corsica tracking campaign, *Mar. Geod.*, *27*, 1–8.
- Gambis, D. (2004), Monitoring Earth orientation using space-geodetic techniques: State-of-the-art and prospective, *J. Geod.*, *78*, 295–305.
- Gruber, T., A. Bode, C. Reigber, P. Schwintzer, R. Biancale, and J.-M. Lemoine (2000), GRIM5-C1: Combination solution of the global gravity field to degree and order 120, *Geophys. Res. Lett.*, *27*, 4005–4008.
- Hefty, J., M. Rothacher, T. Springer, R. Weber, and G. Beutler (2000), Analysis of the first year of Earth rotation parameters with a sub-daily resolution gained at the CODE processing center of the IGS, *J. Geod.*, *74*, 479–487.
- Kouba, J. (2005), Comparison of polar motion with oceanic and atmospheric angular momentum time series for 2-day to Chandler periods, *J. Geod.*, *79*, 33–42.
- Le Provost, C. (2002), FES 2002 - A new version of the FES tidal solution series, paper presented at Jason-1 Science Working Team Meeting, Cent. Natl. d'Etudes Spatiales, Biarritz, France.
- Lieske, J. H., T. Lederle, W. Fricke, and B. Morando (1977), Expressions for the precession quantities based upon the IAU [1976] System of Astronomical Constants, *Astron. Astrophys.*, *58*, 1–16.
- Marini, J. W., and C. W. Murray (1973), Correction of laser range tracking data for atmospheric refraction at elevations above 10 degrees, *Rep. X-591-73-351*, NASA Goddard Space Flight Cent., Greenbelt, Md.
- McCarthy, D. D. (1996), IERS conventions, *IERS Tech. Not.* *21*, Obs. de Paris, Paris.
- McCarthy, D. D., and G. Petit (2004), IERS conventions, *IERS Tech. Not.* *32*, Verlag des Bundesamts für Kartographie und Geod., Frankfurt, Germany.
- Mignard, F. (2004), Overall science goals of the GAIA mission, paper presented at "The Three-Dimensional Universe with GAIA" symposium, Paris Obs., Paris.
- Niell, A. E. (1996), Global mapping function for the atmosphere delay of radio wavelengths, *J. Geophys. Res.*, *101*, 3227–3246.
- Sahin, M., P. A. Cross, and P. C. Sellers (1992), Variance component estimation applied to Satellite Laser Ranging, *Bull. Géod.*, *66*, 284–295.
- Sillard, P., and C. Boucher (2001), Review of algebraic constraints in terrestrial reference frame datum definition, *J. Geod.*, *75*, 63–73.
- Standish, E. M., X. X. Newhall, J. G. Williams, and W. M. Folkner (1995), JPL planetary and lunar ephemerides, *Rep. DE403/LE403*, JPL IOM 314.10-127, Jet Propul. Lab., Pasadena, Calif.
- Wahr, J. M. (1985), Deformation induced by polar motion, *J. Geophys. Res.*, *90*(B11), 9363–9368.
- Watkins, M. M., and R. J. Eanes (1994), Diurnal and semidiurnal variations on Earth orientation determined from LAGEOS laser ranging, *J. Geophys. Res.*, *99*(B9), 18,073–18,079.
- Willis, P., F. G. Lemoine, and L. Soudarin (2007), Looking for systematic error in scale from terrestrial reference frames from DORIS data, in *Dynamic Planet: Monitoring and Understanding a Dynamic Planet With Geodetic and Oceanographic Tools*, edited by P. Tregoning and C. Rizos, *IAG Symp.*, *130*, 143–151.

- Yaya, P. (2002), Apport des combinaisons de techniques astrométriques et géodésiques à l'estimation des paramètres d'orientation de la Terre, Ph.D. thesis, Obs. de Paris, Paris.
- Yoder, C. F., J. G. Williams, and M. E. Parke (1981), Tidal variations of Earth rotation, *J. Geophys. Res.*, *86*, 881–891.
- Zhu, S.-Y., and I. I. Mueller (1983), Effects of adopting new precession, nutation and equinox corrections on the terrestrial reference frame, *Bull. Géod.*, *57*, 29–42.
- 
- P. Berio, Observatoire de la Côte d'Azur, GEMINI/UMR6203-CNRS, avenue Nicolas Copernic, F-06130 Grasse, France. (philippe.berio@obs-azur.fr)
- R. Biancale, Centre National d'Études Spatiales/Observatoire Midi-Pyrénées, DTP/UMR5562-CNRS, 14, avenue Edouard Belin, F-31400 Toulouse, France. (richard.biancale@cnes.fr)
- D. Coulot, Institut Géographique National, ENSG/LAREG, 6 et 8, avenue Blaise Pascal, Cité Descartes, Champs-sur-Marne, F-77455 Marne-la-Vallée cedex 2, France. (david.coulot@ensg.ign.fr)
- A.-M. Gontier, Observatoire de Paris, SYRTE/UMR8630-CNRS, 61, avenue de l'Observatoire, F-75014 Paris, France. (anne-marie.gontier@obspm.fr)
- S. Loyer, Noveltis, Parc Technologique du Canal, 2, avenue de l'Europe, F-31520 Ramonville-Saint-Agne, France. (sylvain.loyer@cnes.fr)
- L. Soudarin, Collecte Localisation Satellites, Parc Technologique du Canal, 8 et 10, rue Hermès, F-31526 Ramonville-Saint-Agne Cedex, France. (laurent.soudarin@cls.fr)